AD-A070 478 MARYLAND UNIV COLLEGE PARK DEPT OF PHYSICS AND ASTRONOMY F/G 20/9
VLASOV EQUILIBRIA FOR A WARM FINITE RADIUS ROTATING RELATIVISTI--ETC(U)
1977 P F OTTINGER, J GUILLORY N00014-75-C-0309
UNCLASSIFIED PUB-77-098 NL

| OF |
AD
A070 478

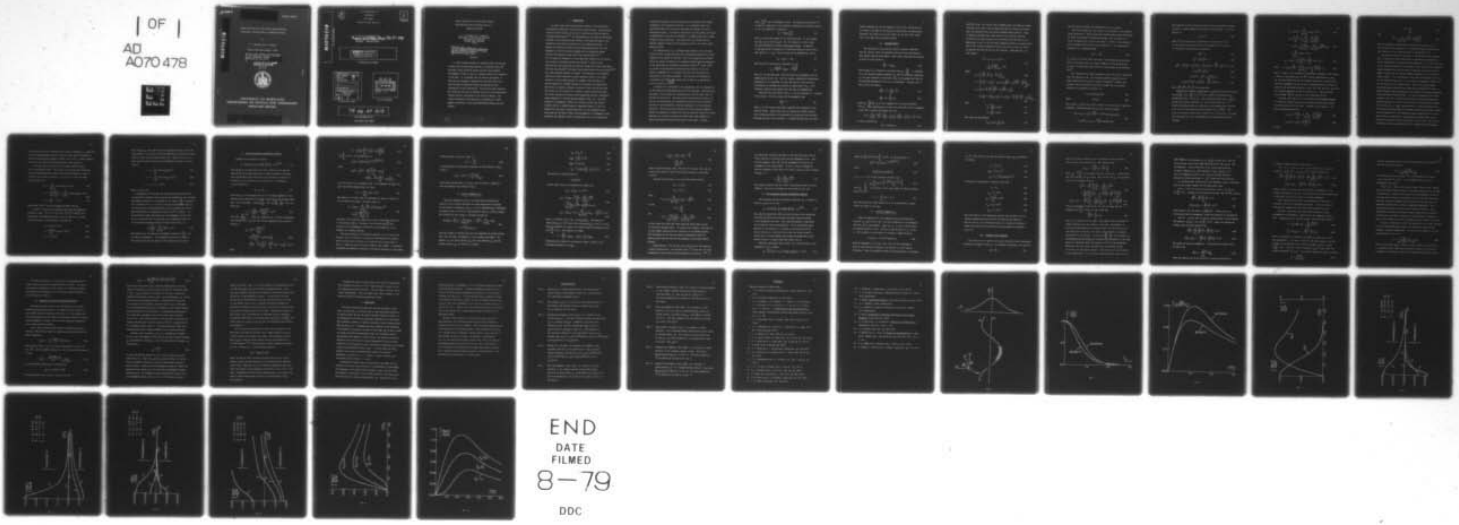

END
DATE
FILMED
8-79
DDC

PREPRINT #609P002

Vlasov Equilibria for a Warm Finite Radius Rotating Relativistic Electron Beam in a Magnetized Plasma

by

P. F. Ottinger and J. Guillory

Physics Publication Number 77-098

Work on this report was supported by ONR Contract N00014-75-C-0309 and/or N00014-67-A-0239 monitored by NRL 6702. 02.

1977

UNIVERSITY OF MARYLAND
DEPARTMENT OF PHYSICS AND ASTRONOMY
COLLEGE PARK, MARYLAND

DDC PROCESSING DATA

PHOTOGRAPH

THIS SHEET

RETURN TO DDA-2 FOR FILE

II
LEVEL

1
INVENTORY

AD A070479

DDC ACCESSION NUMBER

Preprint 609P002, Physics Pub 77-098

DOCUMENT IDENTIFICATION

DISTRIBUTION STATEMENT A
Approved for public release;
Distribution Unlimited

DISTRIBUTION STATEMENT

Accession For
NTIS GRA&I
DDC TAB
Unannounced
Justification
By
Distribution/
Availability Codes
Dist. | Avail and/or special
A

DISTRIBUTION STAMP

DDC
RECEIVED
JUN 28 1979
D

DATE ACCESSIONED

79 06 27 313

DATE RECEIVED IN DDC

PHOTOGRAPH THIS SHEET

Vlasov Equilibria for a Warm Finite Radius Rotating Relativistic Electron Beam in a Magnetized Plasma*

P. F. Ottinger and J. Guillory
Department of Physics and Astronomy
University of Maryland
College Park, Maryland
20742

Work on this report was supported by ONR Contract N00014-75-C-0309 and/or N00014-67-A-0239 monitored by NRL 6702.
02.

Abstract

A Vlasov equilibrium model is developed which can describe a broad class of beam-plasma systems in an applied field, B_z^0. The model treats arbitrary density profiles and azimuthal self-magnetic fields as well as a thermal spread in the momentum of the beam. It is assumed that the electron gyroradius is small but not negligible compared with the beam radius, and that the beam is completely charge neutralized but only fractionally current neutralized. The electron orbit equations are solved and are used to simplify the form of the distribution function and the calculation of its velocity moments. The rotation frequency of the beam and the diamagnetic or paramagnetic properties of such warm beam-plasma systems are also studied.

I. INTRODUCTION

In recent years there has been much interest in the equilibrium and stability properties of relativistic electron beams. One particular reason for this interest is the use of relativistic electron beams as a plasma heating device.[1-8] An understanding of the physical mechanisms involved in this heating process requires a thorough knowledge of the equilibrium and stability properties of the beam-plasma system. In general the stability analyses of such beam-plasma systems that have appeared in the literature have assumed that the background plasma provides both complete charge and current neutralization.[6-13] For the stability analysis it is also generally assumed that the beam is cold as well as spatially uniform and infinite in radial extent. Some work has been done where only partial charge and current neutralization have been assumed[14] and where finite-radius beams have been studied[15-19] but a more complete analysis is needed. The presence of self magnetic fields and radial boundaries can have important effects on the mode structure of beam-plasma systems; for example, their presence can greatly enhance the coupling between the transverse and longitudinal waves that are found by treating a uniform, current neutralized beam. The purpose of this article is to present a Vlasov equilibrium model for a warm relativistic electron beam propagating through a background plasma immersed in a uniform applied magnetic field, B_z. The model allows for self-magnetic fields, for arbitrary radial beam density profiles and for a thermal spread in momentum, however, it will be assumed that the beam is charge neutralized by the background ions. Since $B_\theta \neq 0$ and the beam is warm, both paramagnetic and diamagnetic beam equilibria are possible, where the magnitude of B_θ can be adjusted by

varying the fractional current neutralization provided by the counter-streaming of the background electrons. In a subsequent paper this equilibrium model will be used in analyzing the stability of such a beam-plasma system. It should be pointed out that this model can easily be generalized to describe the problem of a Tokamak plasma with a supra-thermal electron population. Here again both the toroidal and the poloidal magnetic fields can be described as well as the finite radial density profile.

The applied field, B_z, is assumed large enough so that the gyro-radius of both the beam electrons and the background electrons is small compared to the radius of the beam. With this assumption the electron orbits are easily calculated by an expansion method using the smallness of the gyroradius and the method of harmonic balance.[20] These orbits are useful in writing down the distribution functions for the two electron components in a convenient form that will facilitate the calculation of the velocity moments. The ions will be described by a stationary cold fluid model which will be shown to be appropriate for $\omega >> \omega_{ci}$ and $T_i \lesssim \frac{m_i \omega_{ci}^2 r_b^2}{2}$.

In Section II a discussion of the assumptions that are appropriate in describing this beam-plasma system will be presented. Following this discussion, the procedure for calculating the electron orbits will be outlined in Section III. The beam electron distribution function, f_b, and its velocity moments are developed in Sections IV and V, whereas Sections VI and VII provide a similar development for the background electrons. The equations that describe the self-consistent magnetic fields are presented in Section VIII and the numerical solution of these equations are included in Section IX, which gives some examples of typical beam-plasma equilibria described by this model. Finally,

lines, $\frac{v_{\parallel} B_\theta}{B_z}$, and the diamagnetic drift. By requiring the $\underline{E}\times\underline{B}$ drift to be small in comparison to the azimuthal streaming the following condition on the ion temperature is obtained

$$T_i << eB_\theta r_b \left(\frac{n_i}{n_b}\right) \tag{6}$$

Here $v_{\parallel}/c \sim O(1)$ was assumed for the beam electrons. If, for example, $B_\theta \sim 1$ kg, $r_b \sim 1$ cm and $n_i/n_b \sim 25$. Eq. (6) yields $T_i << 7.5$ keV, which is easily satisfied in typical beam-plasma systems. In addition, if the time scale of interest in a stability analysis is much shorter than ω_{ci}^{-1} (i.e., $\omega >> \omega_{ci}$), then the ions can be considered as cold if

$$v_{th} \lesssim \omega_{ci} r_b << \omega r_b \ . \tag{7}$$

This can also be written as a condition on T_i as

$$T_i \lesssim \frac{m_i \omega_{ci}^2 r_b^2}{2} \sim \frac{1}{8} \text{ keV} << \frac{m_i \omega^2 r_b^2}{2} \tag{8}$$

where Eq. (2) has been used. Note that this is in agreement with the example given for Eq. (6). Thus for typical conditions of beam-plasma experiments it is reasonable to treat the ions as a cold fluid for the purposes of studying the stability of waves with $\omega >> \omega_{ci}$. This frequency condition also implies that the ions are unmagnetized.

Since $\underline{E}_0 = 0$ the relativistic factor, γ, for the electrons is a constant of the motion. This fact along with the assumption that

$$\frac{\rho_{e,b}}{r_b} << 1 \tag{9}$$

where ρ_α is the electron gyroradius, simplify the calculation of the electron orbits. These orbits will be invalid for a small fraction of the electrons within a few gyroradii of the axis but will properly describe the bulk of the electrons. It should be noted that the beam

density gradient and the self-magnetic field in the θ direction both are large at the edge of the beam where these orbits are appropriate. Therefore, the effects of the self field, B_θ, and the finite radial size of the beam can be studied in detail.

III. ELECTRON ORBITS

The calculation of the electron orbits is greatly simplified when the electric field is negligible and the electron gyroradius is much smaller than the beam radius. Under these conditions the equation of motion can be written as

$$\gamma \frac{d\underset{\sim}{v}}{dt} = -(\underset{\sim}{v} \times \underset{\sim}{\omega}_{ce}) \tag{10}$$

where $H=\gamma m_e c^2$ is a constant of the motion and $\underset{\sim}{\omega}_{ce} \equiv \frac{e\underset{\sim}{B}}{m_e c}$. In addition to H, the canonical angular momentum, P_θ, and the canonical z-momentum, P_z, are also constants of the motion since it is assumed that there is no functional dependence on the θ or z coordinates. Solving P_θ for $\dot{\theta}$ and P_z for $\dot{z}$ one obtains

$$\gamma \frac{d\theta}{dt} = \gamma\dot{\theta} = \frac{P_\theta}{m_e r^2} + \frac{a_\theta}{r} \tag{11}$$

$$\gamma \frac{dz}{dt} = \gamma\dot{z} = \frac{P_z}{m_e} + a_z \tag{12}$$

where $a_j \equiv \frac{eA_j}{m_e c}$ and A_j is the j component of the vector potential (j=θ,z). These expressions for $\dot{\theta}$ and $\dot{z}$ are then used in the r component of Eq. (10) to obtain an equation for r(t):

$$\gamma^2\ddot{r} = r\left(\frac{P_\theta}{mr^2} + \frac{a_\theta}{r}\right)^2 + \left(\frac{P_z}{m_e} + a_z\right)\omega_{ce}^{\theta} - \left(\frac{P_\theta}{mr} + a_\theta\right)\omega_{ce}^{z} \equiv \bar{F}(r) \tag{13}$$

If r(t) is written as

$$r(t) = R(1+\rho(t)) \ , \tag{14}$$

then $\bar{F}(r)$ in Eq. (13) can be Taylor expanded about r=R using the assumption that $|\rho|<1$, where $|\rho|R$ is identified with the electron gyroradius and R is identified with the electron guiding center position. Again it should be stressed that these orbits do not correctly describe the motion of a small fraction of the electrons near the axis of the beam; there $|\rho| \gtrsim 1$, so that the Taylor expansion would not be appropriate. This is not a serious problem as long as $r_b >> |\rho|R$, so that the orbits do properly describe the bulk of the electrons. Expanding $\bar{F}(r)$, Eq. (13) becomes

$$\gamma^2 \ddot{\rho} = \alpha_0 + \alpha_1 \rho + \alpha_2 \rho^2 + \ldots$$

$$= \sum_{n=0}^{\infty} \frac{\rho^n}{n!} \left. \frac{\partial^n \bar{F}}{\partial r^n} \right|_{r=R} \equiv F(\rho) \tag{15}$$

where

$$\alpha_0 = \left(- \frac{x_\theta^2}{r^2} + \frac{x_\theta}{r} \omega_{ce}^z - \frac{x_z}{r} \omega_{ce}^\theta \right)_{r=R} \tag{16}$$

$$\alpha_1 = \left((\omega_{ce}^z)^2 + (\omega_{ce}^\theta)^2 - 3\alpha_0 + x_\theta \frac{\partial \omega_{ce}^z}{\partial r} - x_z \left(\frac{3\omega_{ce}^\theta}{r} + \frac{\partial \omega_{ce}^\theta}{\partial r} \right) \right)_{r=R} \tag{17}$$

$$\alpha_2 = \left(5\alpha_0 + \frac{x_\theta}{r} \left(\frac{r^2}{2} \frac{\partial^2 \omega_{ce}^z}{\partial r^2} - 2r \frac{\partial \omega_{ce}^z}{\partial r} + \omega_{ce}^z \right) \right.$$

$$\left. - \frac{3}{2} (\omega_{ce}^z)^2 + \frac{3r}{4} \frac{\partial}{\partial r} \left((\omega_{ce}^z)^2 + (\omega_{ce}^\theta)^2 \right) - \frac{x_z}{r} \left(\frac{r^2}{2} \frac{\partial \omega_{ce}^\theta}{\partial r} - 5\omega_{ce}^\theta \right) \right)_{r=R} \tag{18}$$

with

$$x_\theta \equiv \frac{P_\theta}{m_e R} + a_\theta(R) \tag{19}$$

$$x_z \equiv \frac{P_z}{m_e} + a_z(R) \ . \tag{20}$$

Note that the relationship

$$\underset{\sim}{\omega}_{ce} = \underset{\sim}{\nabla} \times \underset{\sim}{a} = \frac{e}{m_e c} \underset{\sim}{\nabla} \times \underset{\sim}{A} \tag{21}$$

has been used in deriving the expressions for α_0, α_1 and α_2.

Since $F(\rho=0)=\alpha_0\neq 0$, Eq. (15) allows for corrections to the guiding center position, R. Unlike traditional guiding center theory which does not treat the problem of streaming electrons, this correction to R can be as large as $0(\varepsilon)$ for the case where $v_{\parallel}/c\sim 0(1)$. The correction can not become of 0(1) since it was assumed $|\rho|<1$. If a generalized potential, V, is defined through

$$F(\rho) = -\frac{\partial V}{\partial \rho} , \tag{22}$$

it is easy to see that this correction to the guiding center position can be attributed in part to a small asymmetry in the potential and in part to a small shift away from $\rho=0$ in the minimum of the potential well.[22]

For convenience the Taylor expansion in Eq. (15) will be terminated after the quadratic term. The resulting nonlinear equation can be solved analytically in terms of elliptic integrals,[23] however that procedure does not provide any physical insight into the solution. Insight can be obtained by writing ρ as

$$\rho = \rho_0+\rho_1\sin\phi+\rho_2\cos 2\phi+\ldots \tag{23}$$

where

$$\phi=\Omega t+\phi_0 . \tag{24}$$

Here $\rho_0\sim 0(\varepsilon)$, $\rho_1\sim 0(\varepsilon)$ and $\rho_2\sim 0(\varepsilon^2)$, where $\varepsilon<<1$ and is used to order the variables. Substituting Eq. (23) into Eq. (15) one obtains

$$\left(\alpha_0 + \alpha_1\rho_0 + \alpha_2\rho_0^2 + \frac{\alpha_2\rho_1^2}{2}\right) + (-\Omega^2\gamma^2+\alpha_1+2\alpha_2\rho_0)\rho_1\sin\phi$$
$$+ \left(-4\Omega^2\gamma^2\rho_2 + \alpha_1\rho_2 - \frac{\alpha_2\rho_1^2}{2}\right)\cos 2\phi+0(\varepsilon^3)=0 \tag{25}$$

This equation can then be solved using the method of harmonic balance. In order to further simplify the solution, each variable, s, will be written as

$$s = \sum_j s^{(j)} \tag{26}$$

where $s^{(j)}$ will denote the contribution to s which is of $0(\varepsilon^j)$. In this manner the solution of Eq. (25) through $0(\varepsilon^2)$ is reduced to solving the following set of equations:

$$\alpha_0^{(0)} = 0 \tag{27}$$

$$\alpha_0^{(1)} + \alpha_1^{(0)}\rho_0^{(1)} = 0 \tag{28}$$

$$\alpha_0^{(2)} + \alpha_1^{(0)}\rho_0^{(2)} + \alpha_1^{(1)}\rho_0^{(1)} + \alpha_2^{(0)}(\rho_0^{(1)})^2 + \frac{\alpha_2^{(0)}}{2}(\rho_1^{(1)})^2 = 0 \tag{29}$$

$$-\gamma^2(\Omega^2)^{(0)} + \alpha_1^{(0)} = 0 \tag{30}$$

$$-\gamma^2(\Omega^2)^{(1)} + \alpha_1^{(1)} + 2\alpha_2^{(0)}\rho_1^{(1)} = 0 \tag{31}$$

$$-4\gamma^2(\Omega^2)^{(0)}\rho_2^{(2)} + \alpha_1^{(0)}\rho_2^{(2)} - \frac{\alpha_2^{(0)}}{2}(\rho_1^{(1)})^2 = 0 \tag{32}$$

where $\rho_0^{(0)} = \rho_1^{(0)} = \rho_2^{(0)} = \rho_2^{(1)} \equiv 0$ by assumption.

Ordering the variables appropriately to describe the beam electrons, one has $\frac{p_{\parallel}}{m_e c} \sim 0(1)$, $\frac{p_{\perp}}{m_e c} \sim 0(\varepsilon)$, $\frac{x_z}{c} \sim 0(1)$ and $\frac{x_\theta}{c} \sim 0(\varepsilon^3)$ along with the assumption of Eqs. (1) and (2). Then setting $\phi(t=0) = \phi_0$ and $\rho_1 = \frac{p_{\perp}}{m_e \gamma \Omega}$ to satisfy the initial conditions, Eq. (15) is solved for $\rho(t)$. It should be mentioned that the correction to the guiding center position, R, is $0(\varepsilon)$ for the ordering considered here (i.e., $\rho_0^{(1)} \neq 0$). This point is discussed in more detail further on in this section. By using this expression for $\rho(t)$, the momentum of the beam electrons can be obtained

$$p_r = p_\perp \cos\phi - \frac{p_\perp^2}{2m_e r\omega_{ce}^z} \sin 2\phi + O(\varepsilon^3) \tag{33}$$

$$p_\theta = \frac{p_\parallel \omega_{ce}^\theta}{\omega_{ce}^z} + \frac{1}{2}\frac{p_\perp^2}{m_e r\omega_{ce}^z} + \frac{p_\parallel^2 (\omega_{ce}^\theta)^2}{m_e r(\omega_{ce}^z)^3}$$
$$+ p_\perp\left(1 + \frac{p_\parallel \omega_{ce}^\theta}{2m_e r(\omega_{ce}^z)^2} - \frac{p_\parallel}{2m_e(\omega_{ce}^z)^2}\frac{\partial\omega_{ce}^\theta}{\partial r}\right)\sin\phi \tag{34}$$
$$+ \frac{p_\perp^2}{2m_e\omega_{ce}^z}\cos 2\phi + O(\varepsilon^3)$$

$$p_z = p_\parallel\left(1 + \frac{1}{2}\left(\frac{\omega_{ce}^\theta}{\omega_{ce}^z}\right)^2\right) - \frac{p_\perp \omega_{ce}^\theta}{\omega_{ce}^z}\sin\phi + O(\varepsilon^3) \tag{35}$$

with $$\phi = \Omega t + \phi_0 = \left(\frac{\omega_{ce}^z}{\gamma} - \frac{p_\parallel \omega_{ce}^\theta}{2m_e r\gamma\omega_{ce}^z}\left(3 + \frac{r}{\omega_{ce}^\theta}\frac{\partial\omega_{ce}^\theta}{\partial r}\right)\right)t + \phi_0 \tag{36}$$

Here $\parallel$ refers to the streaming (ϕ independent) component of the motion, $\perp$ refers to the gyromotion, and $x_z^{(0)}$ has been identified as $p_\parallel/m_e\gamma$. Eq. (15) was solved with all the variables written as functions of R; then the intermediate result for $\underset{\sim}{p}$ was expanded about R=r in order to arrive at the solutions exhibited in Eqs. (33), (34) and (35), where all the variables are again written as function of r. Also note that Ω is not simply $\frac{\omega_{ce}^z}{\gamma}$ but contains a drift correction of $O(\varepsilon)$.

From Eqs. (34) and (35) it is clear that the streaming component of the motion involves both streaming along the field lines as well as a drift across the field lines. Defining a pitch angle, η, for the streaming motion one has

$$p_\parallel \sin\eta = \frac{p_\parallel \omega_{ce}^\theta}{\omega_{ce}^z} + \frac{1}{2}\frac{p_\perp^2}{m_e r\omega_{ce}^z} + \frac{p_\parallel^2 (\omega_{ce}^\theta)^2}{m_e r(\omega_{ce}^z)^3} \tag{37}$$

$$p_\parallel \cos\eta = p_\parallel\left(1 + \frac{1}{2}\left(\frac{\omega_{ce}^\theta}{\omega_{ce}^z}\right)^2\right) \tag{38}$$

so that

$$\eta^{(1)} = \frac{\omega^{\theta}_{ce}}{\omega^{z}_{ce}} \tag{39}$$

and

$$\eta^{(2)} = \frac{1}{m_e p_{\parallel} r\omega^{z}_{ce}} \left(\frac{p_{\perp}^2}{2} + p_{\parallel}^2 \left(\frac{\omega^{\theta}_{ce}}{\omega^{z}_{ce}} \right)^2 \right) \tag{40}$$

Thus the streaming is predominantly along the field lines for the case considered here, however the streaming does depart slightly from this course due to the curvature drift as indicated by $\eta^{(2)}$.

The fact that the $0(\varepsilon)$ correction to the guiding center position, $\rho_0^{(1)}$, is nonzero for this ordering can be explained by consideration of the conservation of canonical angular momentum, P_θ. If each beam electron is injected axially into the plasma at some r=R with zero mechanical angular momentum from a source which is immersed in the axial applied magnetic field, then the canonical angular momentum of the electron is simply $-\omega^{z}_{ce}R^2/2$. The contribution of the axial self-magnetic field to P_θ is not considered here since it is two orders of magnitude smaller than the contribution of the applied field. Now as the electron begins streaming along the helical field lines while gyrating about them, it gains mechanical angular momentum at the expense of the angular momentum associated with the applied field. In terms of anharmonic oscillation potential, Eq. (22), the potential minimum, $\bar{R}$, and the phase-averaged particle position, R, differ in first order, by an amount which depends on the injection $v_{\parallel}$, since the potential is a velocity-dependent one. The rotation associated with the streaming along the field lines accounts for the largest part of the mechanical angular momentum and is of $0(\varepsilon)$. This process is equivalent to saying that the guiding center of the electron is injected at $\bar{R}=R+v_{\parallel}\,\omega^{\theta}_{ce}/(\omega^{z}_{ce})^2$, and not at R. The electron is injected into the potential well at R, displaced from the minimum

at $\bar{R}$; thus the electron oscillates about $\bar{R}$ with a frequency, Ω. Since $V(\rho)$ is not a simple harmonic potential there are also small corrections to the usual electron gyrofrequency as shown in Eq. (36). In what follows R will be used to denote the electron guiding center position.

It is also useful to write down the single particle orbits in the equilibrium fields. These orbits are necessary in calculating the perturbed distribution function when using the method of characteristics in a stability analysis. If $\underset{\sim}{r}'=\underset{\sim}{r}$ at $\tau=t'-t=0$, the beam electron orbits are

$$r' = r + \frac{p_\perp}{m_e \omega_{ce}^z} (\sin\phi - \sin\phi_0) + O(\varepsilon^2) \tag{41}$$

$$\theta' = \theta + \left(\frac{p_\parallel \omega_{ce}^\theta}{m_e \gamma r \omega_{ce}^z}\right)\tau - \frac{p_\perp}{m_e r \omega_{ce}^z} (\cos\phi - \cos\phi_0) + O(\varepsilon^2) \tag{42}$$

$$z' = z + \frac{p_\parallel}{m_e \gamma} \tau + O(\varepsilon^2) \tag{43}$$

where terms of $O(\varepsilon^3)$ have been dropped and where $\phi=\Omega\tau+\phi_0$.

In order to describe the background electrons the following ordering is used: $\frac{v_\parallel}{c} \sim O(\varepsilon^2)$, $\frac{v_\perp}{c} \sim O(\varepsilon^2)$, $\frac{x_z}{c} \sim O(\varepsilon^2)$ and $\frac{x_\theta}{c} \sim O(\varepsilon^3)$ (along with the assumptions found in Eqs. (1) and (2)). In this case the velocity of the electrons is found to be

$$v_r = v_\perp \cos\phi + O(\varepsilon^4) \tag{44}$$

$$v_\theta = \frac{v_\parallel \omega_{ce}^\theta}{\omega_{ce}^z} + v_\perp \sin\phi + O(\varepsilon^4) \tag{45}$$

$$v_z = v_\parallel + O(\varepsilon^4) \tag{46}$$

where $\phi=\omega_{ce}^{z}t+\phi_0$. This shows that the background electrons, which are responsible for the partial current neutralization, essentially stream along the field lines and gyrate about them. Again it is useful to write down the orbits, which for the background electrons are simply given by

$$r' = r + \frac{v_\perp}{\omega_{ce}^{z}} (\sin\phi-\sin\phi_0)+0(\varepsilon^3) \tag{47}$$

$$\theta' = \theta - \frac{v_\perp}{r\omega_{ce}^{z}} (\cos\phi-\cos\phi_0) + 0(\varepsilon^3) \tag{48}$$

$$z' = z + v_{\parallel}\tau + 0(\varepsilon^3) \tag{49}$$

where $\underset{\sim}{r}'=\underset{\sim}{r}$ when $\tau=0$.

Although Eqs. (27) through (32) have only been solved here for two particular orderings, other solutions are possible if the variables are ordered differently. For example if the order of $\frac{\omega_{ce}^{\theta}}{\omega_{ce}^{z}}$ is reduced to $0(\varepsilon^2)$ instead of $0(\varepsilon)$, it is easy to find the new solutions directly from the solutions already discussed by merely changing the ordering where appropriate and dropping any terms of $0(\varepsilon^3)$ or smaller. For the particular example mentioned here, the diamagnetic current will now be of the same order of magnitude as the azimuthal current due to the electron streaming along the helical field lines, i.e.,

$$p_{\parallel}\left(\frac{\omega_{ce}^{\theta}}{\omega_{ce}^{z}}\right) \sim \frac{p_\perp^2}{m_e\gamma\omega_{ce}^{z}} \frac{\partial \ell nn}{\partial r} \sim 0(\varepsilon^2) \tag{50}$$

This implies that the beam can be diamagnetic whereas if $\frac{\omega_{ce}^{\theta}}{\omega_{ce}^{z}} \sim 0(\varepsilon)$ the beam is paramagnetic. The diamagnetic current is of course a fluid propery and does not appear in the single particle orbits.

IV. THE BEAM ELECTRON DISTRIBUTION FUNCTION

Consider the distribution function

$$f_b = N_b(R)\exp\left\{-\frac{1}{T_b}\left[H-\omega_R^b P_\theta-\bar{V}_z^b P_z\right]\right\} \equiv N_b e^{-g_b/T_b} \tag{51}$$

Here ω_R^b can be associated with the fluid rotation of the electron beam and $\bar{V}_z^b$ can be associated with the axial streaming of the beam. Since the guiding center position of the electron is a constant of the motion, N can be written as a function of R. Furthermore, if $p'_{\parallel}$ is defined as

$$p'_{\parallel} \equiv p_{\parallel} - \bar{P}_{\parallel} , \tag{52}$$

such that $\bar{P}_{\parallel}$ is the average value of the streaming component of the momentum and $p'_{\parallel}$ represents the thermal spread about this average value, then γ can be expanded. Assuming $\frac{\bar{P}_{\parallel}}{m_e c} \sim 0(1)$ and $\frac{p'_{\parallel}}{m_e c} \sim \frac{p_\perp}{m_e c} \sim 0(\varepsilon)$ one finds that

$$\gamma = \bar{\gamma} + \frac{p'_{\parallel}\bar{P}_{\parallel}}{\bar{\gamma} m_e^2 c^2} + \frac{p_\perp^2 + p_{\parallel}'^2/\bar{\gamma}^2}{2\bar{\gamma} m_e^2 c^2} + 0(\varepsilon^3) \tag{53}$$

with $\bar{\gamma} \equiv \left(1 + \frac{\bar{P}_{\parallel}^2}{m_e^2 c^2}\right)^{1/2}$. Using this expression for γ and the expressions found in Eqs. (33), (34) and (35) for the components of $\underline{p}$, g_b can be written as

$$\begin{aligned} g_b = {} & mc^2\bar{\gamma} + \frac{p_\perp^2 + p_{\parallel}'^2/\bar{\gamma}^2}{2\bar{\gamma} m_e} \\ & - \omega_R^b r\left(\frac{\bar{P}_{\parallel}\omega_{ce}^\theta}{\omega_{ce}^z} + p_\perp \sin\phi - m_e a_\theta\right) \\ & - \bar{V}_z^b\left(\bar{P}_{\parallel} - \frac{\bar{P}_{\parallel}}{2}\left(\frac{\omega_{ce}^\theta}{\omega_{ce}^z}\right)^2 - \frac{p_\perp \omega_{ce}^\theta}{\omega_{ce}^z}\sin\phi - m_e a_z\right) + 0(\varepsilon^3) \end{aligned} \tag{54}$$

where

$$\bar{P}_{\parallel} \equiv m_e \bar{\gamma}\left(\omega_R^b r \frac{\omega_{ce}^{\theta}}{\omega_{ce}^{z}} + \bar{V}_z^b\left(1 - \frac{1}{2}\left(\frac{\omega_{ce}^{\theta}}{\omega_{ce}^{z}}\right)^2\right)\right) \tag{55}$$

and $\frac{\omega_R^b}{\omega_{ce}^z} \sim 0(\varepsilon)$. By choosing $N_b(R)$ as

$$N_b(R) = \bar{n}_b(R)(2\pi\bar{\gamma}m_e T)^{-3/2} e^{+\bar{g}_b(R)/T_b} \tag{56}$$

where

$$\begin{aligned}\bar{g}_b(R) \equiv \Bigg[mc^2\bar{\gamma} - \omega_R^b R\left(\frac{\bar{P}_{\parallel}\omega_{ce}^{\theta}}{\omega_{ce}^{z}} - m_e a_\theta\right) \\ - \bar{V}_z^b\left(\bar{P}_{\parallel} - \frac{\bar{P}_{\parallel}^2}{2}\left(\frac{\omega_{ce}^{\theta}}{\omega_{ce}^{z}}\right)^2 - m_e a_z\right)\Bigg]_{r=R}\end{aligned} \tag{57}$$

f_b can be written in a convenient form. To accomplish this $\bar{g}_b(R)$ and $n_b(R)$ are Taylor expanded about R=r where

$$R = r - \frac{p_\perp}{m_e \omega_{ce}^z}\sin\phi + 0(\varepsilon^2) \tag{58}$$

Here again it is crucial that the gyroradius be small in comparison to the radius of the beam. The final result is

$$\begin{aligned} f_b \simeq \left(\bar{n}_b(r) - \frac{p_\perp}{m_e\omega_{ce}^z}\frac{\partial\bar{n}_b}{\partial r}\sin\phi\right)(2\pi\bar{\gamma}m_e T_b)^{-3/2} \\ \times \exp\left\{-\frac{p_\perp^2 + p_\parallel'^2/\bar{\gamma}^2}{2\bar{\gamma}m_e T_b}\right\}\end{aligned} \tag{59}$$

where $\bar{n}_b(r)$ is an arbitrary function of r and is obviously identified as the particle density. Moreover, the term involving $\frac{\partial n_b}{\partial r}\sin\phi$ accounts for the diamagnetic current due to the gyromotion in the presence of a density gradient.

The fact that $\bar{n}_b(r)$ is an arbitrary function of r is of particular interest, since it allows one to model any experimentally determined density profile which satisfies the condition that the gyroradius is small in comparison with the density gradient scale length. In Cartesian coordinates an appropriate constant of the motion analogous to the guiding

center position, R (see Eq. (58)), is

$$\xi_x = x - \frac{\gamma v_y}{\omega_{ce}} \quad . \tag{60}$$

In this geometry the appropriate expansion for some function, $h(\xi_x)$, would be

$$h(\xi_x) \sim h(x) + \left(-\frac{\gamma v_y}{\omega_{ce}}\right) \frac{\partial h}{\partial \xi_x}\bigg|_{\xi_x = x} \tag{61}$$

where again the gyroradius, $|\gamma v_y/\omega_{ce}|$, must be small in comparison with the gradient scale length of $h(\xi_x)$.

V. VELOCITY MOMENTS OF f_b

Using the expression (59) for the beam electron distribution function, one can easily determine the fluid properties of the beam. For the sake of convenience, the $p_{\parallel}$, $p_{\perp}$ and ϕ momentum space coordinates introduced in Sec. III will be used instead of the p_r, p_θ and p_z system. The Jacobian for this change of variables is given by

$$dp_r dp_\theta dp_z = \left\{ p_\perp \left[1 + \frac{p_{\parallel}}{2m_e r(\omega_{ce}^z)^2} \left(\omega_{ce}^\theta - r \frac{\partial \omega_{ce}^\theta}{\partial r} \right) - \frac{p_\perp}{m_e r \omega_{ce}^z} \sin\phi \right] + O(\epsilon^3) \right\} dp_\perp dp_{\parallel} \, d\phi \tag{62}$$

With this change of variables and with the components of $\underset{\sim}{p}$ given in Eqs. (33), (34) and (35), the moments of f_b are readily calculated. The density, n_b, the fluid velocity, $\underset{\sim}{V}_b$, the fluid momentum, $\underset{\sim}{P}_b$, and the pressure tensor, $\underset{\sim}{\Pi}_b$, are defined as follows:

$$n_b = \int f_b \, d^3p \tag{63}$$

$$n_b \underset{\sim}{V}_b = \int \frac{\underset{\sim}{p}}{m_e \gamma} f_b \, d^3p \tag{64}$$

$$n_b \underset{\sim}{P}_b = \int \underset{\sim}{p} \, f_b \, d^3p \tag{65}$$

$$\underset{\sim}{\Pi}_b = \int (\underset{\sim}{p} - \underset{\sim}{P}_b) \left(\frac{\underset{\sim}{p}}{m_e \gamma} - \underset{\sim}{V}_b \right) f_b \, d^3p \, . \tag{66}$$

The density is trivially given by

$$n_b(r) = \bar{n}_b(r)$$

and the fluid velocity and momentum are found to be

$$P_{br} = m_e \bar{\gamma} V_{br} = 0 + 0(\varepsilon^3) \tag{67}$$

$$P_{b\theta} = m_e \bar{\gamma} V_{b\theta} = \frac{\bar{P}_{\parallel} \omega_{ce}^{\theta}}{\omega_{ce}^{z}} - \frac{p_{th}^2}{2 m_e \omega_{ce}^{z}} \frac{\partial \ell n n_b}{\partial r} + \frac{\bar{P}_{\parallel}^2 \omega_{ce}^{\theta}}{m_e r (\omega_{ce}^{z})^3} \left(\frac{3\omega_{ce}^{\theta}}{2} - \frac{r}{2} \frac{\partial \omega_{ce}^{\theta}}{\partial r} \right) + 0(\varepsilon^3) \tag{68}$$

$$P_{bz} = m_e \bar{\gamma} V_{bz} = \bar{P}_{\parallel} + \frac{\bar{P}_{\parallel}^2}{2 m_e r (\omega_{ce}^{z})^2} \left(\omega_{ce}^{\theta} - r \frac{\partial \omega_{ce}^{\theta}}{\partial r} \right) + 0(\varepsilon^2) \tag{69}$$

where $\bar{\gamma}$ is defined in Eq. (53), and $p_{th}^2 \equiv 2 m_e \bar{\gamma} T_b$. The reason for calculating $P_{b\theta}$ to $0(\varepsilon^3)$ while only calculating P_{bz} to $0(\varepsilon^2)$ is clear where one examines the radial force balance equation, keeping in mind that $\frac{\omega_{ce}^{\theta}}{\omega_{ce}^{z}} \sim 0(\varepsilon)$. This equation is simply

$$0 = - \frac{P_{b\theta}^2}{m_e r} + \omega_{ce}^{z} P_{b\theta} - \omega_{ce}^{\theta} P_{bz} + \frac{\bar{\gamma}}{n_b} [\underset{\sim}{\nabla} \cdot \underset{\sim}{\Pi}_b]_r \tag{70}$$

Calculating the elements of the pressure tensor, results in the following expression for $[\underset{\sim}{\nabla} \cdot \underset{\sim}{\Pi}_b]_r$

$$[\nabla\cdot\underset{\sim}{\underset{\sim}{\Pi}}_b]_r = \frac{1}{r}\frac{\partial}{\partial r}(r\Pi_b^{rr}) - \frac{\Pi_b^{\theta\theta}}{r}$$

$$= \frac{p_{th}^2}{2m_e\bar{\gamma}}\frac{\partial n_b}{\partial r} \tag{71}$$

Thus by substituting Eqs. (68), (69) and (71) into Eq. (70), one can easily verify that the radial force balance equation is satisfied to $O(\varepsilon^3)$.

Defining a pitch angle, ξ, for the fluid motion one has

$$P_{b\theta} = P_{\parallel}\sin\xi \tag{72}$$

$$P_{bz} = P_{\parallel}\cos\xi \tag{73}$$

where

$$P_{\parallel} \equiv \bar{P}_{\parallel} + \frac{\bar{P}_{\parallel}^2}{2m_e r(\omega_{ce}^z)^2}\left(\omega_{ce}^{\theta} - r\frac{\partial\omega_{ce}^{\theta}}{\partial r}\right) , \tag{74}$$

so that

$$\xi^{(1)} = \frac{\omega_{ce}^{\theta}}{\omega_{ce}^z} \tag{75}$$

and

$$\xi^{(2)} = \frac{\bar{P}_{\parallel}^2(\omega_{ce}^{\theta})^2}{m_e P_{\parallel} r(\omega_{ce}^z)^3} - \frac{p_{th}^2}{2m_e P_{\parallel}\omega_{ce}^z}\frac{\partial \ell n n_b}{\partial r} \tag{76}$$

To first order the fluid also flows along the field lines, as did the electron's guiding center. To second order, however, the motion of a fluid element differs from the trajectory of the guiding centers. This difference arises from the electron's gyromotion about the guiding center position and from the presence of the radial density gradient.

Considering Eqs. (75) and (76), the fluid motion of the beam has a simple interpretation. As mentioned above $\xi^{(1)}$ shows that the fluid predominantly flows along the helical magnetic field lines. $\xi^{(2)}$, on

the other hand, describes the shear of the fluid flow away from the field lines due to curvature drift and the diamagnetic drift. Thus the self magnetic field, B_z^s, will be paramagnetic as long as the diamagnetic drift remains small. In order to have a diamagnetic beam the diamagnetic drift must be at least as large as this streaming along $\underset{\sim}{B}$, i.e.,

$$P_{\parallel} \frac{\omega_{ce}^{\theta}}{\omega_{ce}^{z}} \lesssim \frac{p_{th}^2}{2m_e \omega_{ce}^{z}} \frac{\partial \ell n n_b}{\partial r} \tag{77}$$

This usually requires that the current neutralization must be fairly complete. This will be discussed in more detail in Sec. VIII.

VI. THE BACKGROUND ELECTRON DISTRIBUTION FUNCTION

The background electron distribution function, f_e, is similar in form to f_b given in Eq. (51)

$$f_e = N_e(R) \exp\left\{-\frac{1}{T_e}\left[H - \omega_R^e P_\theta - \bar{V}_z^e P_z\right]\right\} \equiv N_e e^{-g_e/T_e} \tag{78}$$

Here ω_R^e can be associated with the fluid rotation of the background electrons and $\bar{V}_z^b$ can be associated with axial counterstreaming of the background electrons. This counterstreaming is responsible for the partial current neutralization. Since the guiding center position of the electron is a constant of the motion N_e and $\bar{V}_z^e$ must be written as a function of R so that the return current is restricted to the beam channel even though the background electron density varies on a length scale much longer than r_b.

Using the expressions found in Eqs. (44), (45) and (46) for the components of $\underset{\sim}{v}$, g_e becomes

$$g_e = \frac{m_e}{2}\left[v_\perp^2 + (v_\parallel - V_\parallel)^2 + 2r\omega_R^e a_\theta + 2a_z \bar{V}_z^e - V_\parallel^2\right] + O(\epsilon^5) \tag{79}$$

where $V_{\parallel} \equiv \bar{V}_z^e(r)+0(\varepsilon^4)$ and $\frac{\omega_R^e}{\omega_{ce}^z} \sim 0(\varepsilon^3)$. By choosing $N_e(R)$ as

$$N_e(R) = \bar{n}_e(2\pi m_e T_e)^{-3/2} e^{+\bar{g}_e(R)/T_e} \tag{80}$$

where

$$\bar{g}_e(R) = 2R\omega_R a_\theta + 2a_z \bar{V}_z^e - V_{\parallel}^2 \tag{81}$$

f_e can be written in the following convenient form,

$$f_e \simeq \frac{\bar{n}_e}{(2\pi m_e T_e)^{3/2}} \exp\left\{ - \frac{v_\perp^2 + (v_\parallel - V_\parallel(r))^2}{v_{th}^2} \right\} \tag{82}$$

with $v_{th}^2 \equiv \frac{2T_e}{m_e}$. In arriving at this result $\bar{g}_e(R)$ was Taylor expanded about R=r where

$$R = r - \frac{v_\perp}{\omega_{ce}^z} \sin\phi + 0(\varepsilon^3) \tag{83}$$

Note that $\bar{n}_e$ may be a weak function of r but is essentially constant across the radius of the beam.

VII. VELOCITY MOMENTS OF f_e

Using the expression for the background electron distribution function, f_e, given by Eq. (82), the fluid properties of the background electrons can be investigated. Again the $v_\parallel$, $v_\perp$ and ϕ velocity space coordinates developed in Sec. III will be used in place of v_r, v_θ and v_z. The Jacobian for this change of variables is simply given by

$$dv_r dv_\theta dv_z = [v_\perp + 0(\varepsilon^4)] dv_\perp dv_\parallel d\phi \tag{84}$$

With the components of $\underset{\sim}{\chi}$ in Eqs. (44), (45) and (46) expressed in terms of these natural coordinates, the moments of f_e are readily calculated. Since the background plasma is nonrelativistic, the density,

n_e, the fluid velocity, $\underset{\sim}{V}_e$, and the pressure tensor, $\underset{\sim}{\underset{\sim}{\Pi}}_e$, are defined as follows:

$$n_e = \int f_e \, d^3v \tag{85}$$

$$n_e \underset{\sim}{V}_e = \int \underset{\sim}{v} \, f_e \, d^3v \tag{86}$$

$$\underset{\sim}{\underset{\sim}{\Pi}}_e = m_e \int (\underset{\sim}{v}-\underset{\sim}{V}_e)(\underset{\sim}{v}-\underset{\sim}{V}_e) f_e d^3v \tag{87}$$

Performing the appropriate integrations one finds

$$n_e = \bar{n}_e \tag{88}$$

$$V_{er} = 0 + 0(\varepsilon^4) \tag{89}$$

$$V_{e\theta} = \frac{V_{\parallel} \omega^{\theta}_{ce}}{\omega^{z}_{ce}} + 0(\varepsilon^4) \tag{90}$$

$$V_{ez} = V_{\parallel} + 0(\varepsilon^4) \tag{91}$$

$$\underset{\sim}{\underset{\sim}{\Pi}}_e = 0 + 0(\varepsilon^4) \tag{92}$$

Thus fluid motion of the background electron only involves the slow counterstreaming along $\underset{\sim}{B}$; all other fluid motions are ignorable. The fact that $V_{\parallel}$ is an arbitrary function of r allows the freedom to choose the return current profile and thus determine the dependence of B_θ on r.

VIII. MAGNETIC FIELD EQUATIONS

The result of Sec. V and VII can now be utilized to self consistently determine the magnetic field, $\underset{\sim}{B}$. From Maxwell's equations, $\underset{\sim}{B}$ is given by

$$\underset{\sim}{\nabla}\times\underset{\sim}{B} = \frac{4\pi}{c} \underset{\sim}{J} \tag{93}$$

where $\underset{\sim}{J}$ is current produced by the fluid motion of the electrons. Since the ions are stationary, Eq. (93) simply becomes

$$\underset{\sim}{\nabla}\times\underset{\sim}{\omega}_{ce} = -\left(\frac{\omega_{pb}^2}{c^2}\underset{\sim}{V}_b + \frac{\omega_{pe}^2}{c^2}\underset{\sim}{V}_e\right) \tag{94}$$

where $\omega_{p\alpha}^2 \equiv \frac{4\pi n_\alpha e^2}{m_e}$ is the plasma frequency of species α. Substituting Eqs. (68) and (69) for $\underset{\sim}{V}_b$ and Eqs. (90) and (91) for $\underset{\sim}{V}_e$, the equations for the two components of $\underset{\sim}{B}$ are

$$\begin{aligned} +\frac{\partial\omega_{ce}^z}{\partial r} = +\frac{\omega_{pb}^2}{c^2}\Bigg[&\frac{\bar{P}_{\parallel}\,\omega_{ce}^\theta}{m_e\omega_{ce}^z\bar{\gamma}} - \frac{p_{th}^2}{2m_e^2\bar{\gamma}\omega_{ce}^z}\frac{\partial \ell n n_b}{\partial r} \\ &+ \frac{\bar{P}_{\parallel}^2(\omega_{ce}^\theta)^2}{2m_e^2\bar{\gamma}r(\omega_{ce}^z)^3}\left(3 - \frac{r}{\omega_{ce}^\theta}\frac{\partial\omega_{ce}^\theta}{\partial r}\right)\Bigg] + \frac{\omega_{pe}^2}{c^2}\left(\frac{V_{\parallel}\,\omega_{ce}^\theta}{\omega_{ce}^z}\right) \end{aligned} \tag{95}$$

$$\frac{1}{r}\frac{\partial}{\partial r}(r\omega_{ce}^\theta) = -\frac{\omega_{pb}^2}{c^2}\left[\frac{\bar{P}_{\parallel}}{m_e\bar{\gamma}} + \frac{\bar{P}_{\parallel}^2\,\omega_{ce}^\theta}{2m_e^2\bar{\gamma}r(\omega_{ce}^z)^2}\left(1 - \frac{r}{\omega_{ce}^\theta}\frac{\partial\omega_{ce}^\theta}{\partial r}\right)\right] + \frac{\omega_{pe}^2}{c^2}[V_{\parallel}] \tag{96}$$

Using the assumptions found in Eqs. (1) and (2) along with the assumption that $\frac{\bar{P}_{\parallel}}{m_e c} \sim 0(1)$, Eq. (96) shows that

$$\frac{r_b^2\omega_{pb}^2}{c^2} = \frac{r_b^2}{r_s^2} \lesssim 0(\varepsilon) \tag{97}$$

where r_s is skin depth of the beam. This implies that the fields can readily penetrate into the interior of the beam. Furthermore, if the current neutralization is considered poor, the first term on the right hand side of both Eq. (95) and Eq. (96) provides the dominant contribution to the current. In this case $\frac{\omega_{Pb}^2}{\omega_{pe}^2} = \frac{n_b}{n_e} \sim 0(\varepsilon)$; however, if the background plasma density is increased (or equivalently if the beam density is decreased) while $\frac{V_{\parallel}}{c}$ remains of $0(\varepsilon^2)$ for the background electrons, then the current neutralization is improved although it is still not necessarily complete. When this occurs the situation is more complicated. If the current neutralization is improved (e.g.,

$\lesssim$50% complete) by increasing n_e, but $\omega^{\theta}_{c\theta}/\omega^{z}_{c\theta}$ is still $0(\varepsilon)$, then the first and last terms on the right hand side of Eq. (95) and Eq. (96) are important. On the other hand if the current neutralization is nearly complete (e.g., $\gtrsim$90% complete) so that $\omega^{\theta}_{ce}/\omega^{z}_{ce} \sim 0(\varepsilon^2)$, then the diamagnetic current in Eq. (95) also becomes important, whereas the terms proportional to $(\omega^{\theta}_{ce})^2$ become even less important.

To illustrate more clearly some of the different types of equilibria that can be treated consider the following three cases:

Case i) - Here the current neutralization is poor, $\omega^{\theta}_{ce}/\omega^{z}_{ce} \sim 0(\varepsilon)$ and $\frac{n_b}{n_e} \sim 0(\varepsilon)$. Keeping only the leading terms Eqs. (95) and (96) reduce to

$$\frac{\partial \omega^{z}_{ce}}{\partial r} = \frac{\omega^{2}_{pb}}{c^2} \frac{\omega^{\theta}_{ce}}{\omega^{z}_{ce}} \bar{V}^{b}_{z} + 0(\varepsilon^3) \tag{98}$$

$$\frac{1}{r} \frac{\partial}{\partial r} (r\omega^{\theta}_{ce}) = - \frac{\omega^{2}_{pb}}{c^2} \bar{V}^{b}_{z} + 0(\varepsilon^2) \tag{99}$$

where from Eq. (55) one has $\bar{P}_{\parallel} \simeq m_e \bar{\gamma} \bar{V}^{b}_{z} + 0(\varepsilon^2)$. Since there is no contribution from the diamagnetic current the beam will be paramagnetic.

Case ii) - In this case the current neutralization is approximately 50% complete, $\omega^{\theta}_{ce}/\omega^{z}_{ce} \sim 0(\varepsilon)$ and $\frac{n_b}{n_e} \sim 0(\varepsilon^2)$. Again only keeping the leading terms the field equations are

$$\frac{\partial \omega^{z}_{ce}}{\partial r} = \frac{\omega^{\theta}_{ce}}{\omega^{z}_{ce}} \left(\frac{\omega^{2}_{pb}}{c^2} \bar{V}^{b}_{z} + \frac{\omega^{2}_{pe}}{c^2} \bar{V}^{e}_{z} \right) + 0(\varepsilon^3) \tag{100}$$

$$\frac{1}{r} \frac{\partial}{\partial r} (r\omega^{\theta}_{ce}) = - \left(\frac{\omega^{2}_{pb}}{c^2} \bar{V}^{b}_{z} + \frac{\omega^{2}_{pe}}{c^2} \bar{V}^{e}_{z} \right) + 0(\varepsilon^2) \tag{101}$$

Here again the beam is paramagnetic. One particularly simple choice for $\bar{V}^{e}_{z}$ is just

$$\bar{V}^{e}_{z}(r) = - \frac{\omega^{2}_{pb}(r)}{\omega^{2}_{pe}} \bar{V}^{b}_{z} F_N \tag{102}$$

where F_N = constant and is the fraction of current neutralization.

In general, however, F_N may be function of r.

Case iii) - In this case the current neutralization is nearly complete, $\omega^{\theta}_{ce}/\omega^{z}_{ce} \sim 0(\varepsilon^2)$ and $n_b/n_e \sim 0(\varepsilon^2)$. Here one finds that

$$\frac{\partial \omega^{z}_{ce}}{\partial r} = \frac{\omega^{\theta}_{ce}}{\omega^{z}_{ce}} \left(\frac{\omega^{2}_{pb}}{c^2} \bar{V}^{b}_{z} + \frac{\omega^{2}_{pe}}{c^2} \bar{V}^{e}_{z} \right) - \frac{\omega^{2}_{pb}}{c^2} \frac{p^{2}_{th}}{2m_e^{2-\gamma}\omega^{z}_{ce}} \frac{\partial \ell n n_b}{\partial r} + 0(\varepsilon^4) \qquad (103)$$

$$\frac{1}{r} \frac{\partial}{\partial r} (r\omega^{\theta}_{ce}) = - \left(\frac{\omega^{2}_{pb}}{c^2} \bar{V}^{b}_{z} + \frac{\omega^{2}_{pe}}{c^2} \bar{V}^{e}_{z} \right) + 0(\varepsilon^3) \qquad (104)$$

From Eq. (103) it is clear that the beam may be diamagnetic if the current neutralization is good. Of course if the current neutralization is very good, $\omega^{\theta}_{ce} \sim 0$ and the beam is obviously diamagnetic.

These three cases illustrate the flexibility of this model in treating a variety of beam-plasma equilibria. In the next Section some specific examples will be presented for these three cases.

One other interesting case arises when the beam is neither paramagnetic nor diamagnetic, implying that the azimuthal current is zero. Consequently B_z is uniform and Eqs. (103) and (104) reduce to

$$0 = \omega^{\theta}_{ce}(r)\bar{V}^{b}_{z}(1-F_N) - \frac{p^{2}_{th}}{2m_e^{2-\gamma}} \frac{\partial \ell n n_b(r)}{\partial r} \qquad (105)$$

$$\frac{1}{r} \frac{\partial}{\partial r} (r\omega^{\theta}_{ce}(r)) = - \frac{\omega^{2}_{pb}(r)}{c^2} \bar{V}^{b}_{z}(1-F_N) \qquad (106)$$

where it is assumed for simplicity that $\bar{V}^{e}_{z}(r)$ is given by Eq. (102) with F_N=constant. It is easy to show that the other terms in Eqs. (95) and (96) can be ignored for all values of F_N when $J_{\theta} \lesssim 0(\varepsilon^3)$ as long as $\frac{\bar{P}_{\parallel}}{m_e c} \sim 0(1)$. Using Eq. (105) to eliminate $\omega^{\theta}_{ce}(r)$ in Eq. (106), one obtains an equation for $n_b(r)$. Solving this equation for $n_b(r)$ one finds

$$n_b = \frac{n_b(0)}{(1+r^2/r_b^2)^2} \qquad (107)$$

which is the density profile derived from the Bennett distribution[25,26] where the beam radius must be

$$\bar{r}_b = \frac{2c\ p_{th}}{\omega_{pb}(0)\bar{V}_z^b m_e \bar{\gamma}^{1/2}(1-F_N)} \tag{108}$$

If the beam radius is not equal to $\bar{r}_b$, then $dB_z/dr \neq 0$ even though $n_b(r)$ is given by Eq. (107). B_z is diamagnetic when $r_b < \bar{r}_b$ and paramagnetic when $r_b > \bar{r}_b$.

If $F_N=0$ (i.e., there is no return current), then B_z=const. implies that the azimuthal fluid velocity of the beam vanishes so that the beam is nonrotating. Physically this means that the diamagnetic current of the beam exactly cancels the azimuthal current of the beam associated with the electrons streaming along the helical field lines (plus any azimuthal particle drifts, which are generally negligible). This cancellation persists across the entire profile of the beam. Fig. 1 illustrates this point by showing a typical beam electron trajectory. In particular, the sense of rotation of the gyromotion is opposite to that of the rotation due to the streaming along the helical field lines.

If $n_b(r)$ is given by Eq. (107) but F_N=const.$\neq 0$, it is still possible to have a nonrotating beam, however the rotation of return current produces a residual diamagnetism. In this case the radius of the nonrotating beam is found to be

$$\tilde{r}_b = \frac{2c\ p_{th}}{\omega_{pb}(0)\bar{V}_z^b m_e \gamma^{1/2}(1-F_N)^{1/2}} \tag{109}$$

Note that when $F_N=0$, $\tilde{r}_b=\bar{r}_b$. Finally if F_N is chosen as a function of r, equilibria can be found with B_z=constant, however, $n_b(r)$ will not correspond to the Bennett profile and in general the beam will rotate.

From this discussion, it is clear that a nonrotating beam is a rather special case and that beams generally do rotate. Of course, the physical consequences of this rotation in a stability analysis will depend on the magnitude of the rotation frequency compared to the time scale of interest.

IX. EXAMPLES OF TYPICAL BEAM-PLASMA EQUILIBRIA

Two density profiles that will be considered are the Bennett profile and the Gaussian profile. The Bennett profile, however, is more diffuse than the Gaussian profile (Fig. 2). This implies that the steeper gradients at the edge of the Gaussian profile will produce larger diamagnetic currents. This will have important consequences for the beam rotation frequency.

If Eq. (102) is used for $\bar{V}_z^e(r)$ where for simplicity F_N=const., then Eqs. (99), (101) and (104) are mathematically equivalent and are easily integrated:

$$\omega_{ce}^{\theta}(r) = -\frac{1}{r}\int_0^r \frac{\omega_{pb}^2(r')}{c^2}\bar{V}_z^b(1-F)r'dr' \tag{110}$$

where F_N=0 for case i, $F_N \sim .5$ for case ii and $F_N \gtrsim .9$ for case iii of Sec. VIII. For the Bennett profile, Eq. (107), this can be integrated to give

$$\omega_{ce}^{\theta}(r) = -\frac{\omega_{pb}^2(0)\bar{V}_z^b(1-F_N)}{2c^2}\frac{r}{(1+r^2/r_b^2)} \quad . \tag{111}$$

For the Gaussian profile $n_b(r)$ is expressed as

$$n_b(r) = n_b(0)\exp\{-r^2/r_b^2\} \tag{112}$$

and the solution of Eq. (110) for this case is just

$$\omega_{ce}^{\theta}(r) = -\frac{\omega_{pb}^2(0)\bar{V}_z^b(1-F_N)}{2C^2}\,\frac{r_b^2(1-\exp\{-r^2/r_b^2\})}{r} \tag{113}$$

Note that in both cases $\omega_{ce}^{\theta}(r)$ increases linearly with r near the center of the beam ($r<<r_b$), and falls off like r^{-1} outside the beam ($r>>r_b$). ω_{ce}^{θ} is plotted as a function of r in Fig. 3, where for comparison the density on axis, $n_b(0)$, and the beam radius, r_b, are set equal for the two different profiles. Although the total current is the same for both profiles, the peak value of B_θ is ∿25% higher for the Gaussian profile than for the Bennett profile simply because the Bennett profile is more diffuse. By choosing F_N appropriately, the curves will correspond to any one of three cases discussed in Sec. VIII. With certain values for the parameters this model can properly describe self fields as large as ∿10% of the applied field for a Gaussian profile (Fig. 4). B_θ could become even larger for a density profile with a sharper boundary than the Gaussian profile.

Turning to the case where $J_\theta \simeq 0$, it is interesting to examine how the axial self magnetic field, B_z^s, and the beam rotation frequency, ω_R, are modified by varying r_b. Here the beam rotation frequency, ω_R, is defined as

$$\omega_R = \frac{V_\theta(r)}{r} \tag{114}$$

If $r_b=\bar{r}_b$ then B_z^s will vanish for all r, and if $r_b=\tilde{r}_b$ then ω_R will vanish for all r. $B_z^s(r)$ and $\omega_R(r)$ are plotted in Figs. (5) and (6) for four different values of r_b where the beam density follows a Bennett profile. Observe that the diamagnetic beams are thinner and generally rotate faster near the axis than the paramagnetic beams. Although $F_N=0.5$, the diamagnetic beams considered here differ from the paramagnetic beams of case ii in Sec. VIII because the beam

radius is smaller. Figs. (7) and (8) display the corresponding curves for $B_z^s(r)$ and $\omega_R(r)$ when $n_b(r)$ follows a Gaussian profile. Note that $\omega_R(r)$ depends critically on the shape of the density profile while B_z^s only has a weak dependence on $n_b(r)$. In particular, the beam rotates in the same direction across the entire profile of the beam for the Bennett case for any r_b, whereas the beam can change its direction of rotation at the outer edge of the beam for certain values of r_b when the density profile is Gaussian. Although the behavior of $B_z^s(r)$ about $r_b=\bar{r}_b$ is interesting its magnitude is small compared to the applied field since it was assumed that $\omega_{ce}^{\theta}/\omega_{ce}^{z} \lesssim 0(\varepsilon)$ and $\frac{p_{th}}{m_e c} \lesssim 0(\varepsilon)$. Larger values of $p_{th}/m_e c$ or $\omega_{ce}^{\theta}/\omega_{ce}^{z}$ will of course make these effects more important.

If the current neutralization is better in the interior of the beam than at the edge of the beam, then a larger portion of the net current flows on the surface of the beam. This situation can arise when $r_b\omega_{pe}/c>1$ and the return current has not yet diffused out of the beam channel.[27,28] This situation is easily modeled by allowing F_N to be a function of r. One convenient choice is

$$F_N(r) = \bar{F}_N n_b(r)/n_b(0)$$

Figs. (9) and (10) show the effect that this has on $B_\theta(r)$ for the Bennett profile and the Gaussian profile respectively for different values of $\bar{F}_N$. When $\bar{F}_N \simeq 1$, B_θ still reaches an appreciable peak value since the current is only completely neutralized at the center of the beam. Furthermore with the current flowing nearer to the edge of the beam, B_θ peaks further from the center of the beam than if $F_N(r)$ were constant.

Although the choice of $F_N(r)$ given in Eq. (115) is instructive, any reasonable function of r can be used for $F_N(r)$ in order to fit any appropriate profile for $B_\theta(r)$. Thus both $n_b(r)$ and $B_\theta(r)$ can be chosen independently. This fact makes this Vlasov treatment a very powerful method for modeling beam-plasma systems.

X. CONCLUSIONS

The Vlasov equilibrium model that has been developed in this paper can describe a very broad class of warm beam-plasma systems in an applied field, B_z^0; but the entire treatment depends crucially on the smallness of the electron gyroradius compared to the beam radius. This condition, however, is easily satisfied in typical systems where $B_z^0 \gtrsim 1$ kg and $r_b \gtrsim 1$ cm. Assuming that this condition on the gyroradius is satisfied, the procedure outlined in this paper can be used to model any charge neutralized beam-plasma system with reasonable density and azimuthal self magnetic field profiles. The density profile and azimuthal field profile can be chosen independently since the theta component of the $\nabla\times\underset{\sim}{B}$ equation can be satisfied by adjusting the fractional current neutralizational factor, $F_N(r)$. In other words the $(\nabla\times\underset{\sim}{B})_\theta$ equation can be used to determine $F_N(r)$ given the functional dependence of n_b and B_θ on r. Of course, if $F_N(r)$ is known, then the equation can be used to find $B_\theta(r)$.

By making the simple choice of $F_N(r)$=const. and using the $\nabla\times\underset{\sim}{B}$ equation to solve for $B_\theta(r)$ and $B_z(r)$, it was possible to investigate the dependence of the beam rotation frequency, $\omega_R(r)$, and the axial self magnetic field, $B_z^s(r)$, on the density profile of the beam, $n_b(r)$, and the fraction of current neutralization, F_N. When $F_N > 0.5$ it was

found that B_z^s can be diamagnetic for a sufficiently warm beam but when $F_N<0.5$, B_z^s was paramagnetic. In general diamagnetic beams were also found to be thinner than paramagnetic beams because of the increased pinching force when $J_\theta<0$. It was discovered that ω_R depends strongly on the shape of the density profile and that the Bennett profile with radius $\tilde{r}_b$ (Eq. 109) corresponds to the case of a nonrotating beam, i.e., $\omega_R(r)=0$ for all r. However, this nonrotating beam is only one special case of the general type of beam-plasma systems described by this equilibrium model.

Because of the flexibility in the choice of $n_b(r)$ and $B_\theta(r)$ mentioned above, this equilibrium model will be very valuable for studying the effects of self magnetic fields and radial inhomogeneities on the stability of beam plasma system. Since the model also allows for a thermal spread in momentum, thermal effects on the stability of such systems can also be studied. Furthermore, as mentioned in Sec. III, the beam electron orbits found in Eqs. (41), (42) and (43) and background electron orbits found in Eqs. (47), (48) and (49) can be utilized in calculating the perturbed distribution functions for a stability analysis using the method of characteristics. This analysis will be the subject of a future paper.

FIGURE CAPTIONS

Fig. 1 Trajectory of a typical beam electron. The beam electron gyrates about $\underset{\sim}{B}$ in the opposite sense that it rotates about the z-axis while streaming along $\underset{\sim}{B}$.

Fig. 2 Beam density, $n_b(r)$, as a function of the radial position, r. Both Bennett and Gaussian profiles are shown, with $\omega_{pb}(0)$ and r_b identical for both cases.

Fig. 3 Azimuthal self-magnetic field, $B_\theta(r)$, as a function of the radial position, r. Here the fractional current neutralization, F_N, is a constant ($0 \leq F_N \leq 1$). Examples of the three cases discussed in Sec. VIII are obtained when $F_N \lesssim 0.1$ (case i), $F_N \sim 0.5$ (case ii) and $F_N \gtrsim 0.9$ (case iii). The parameters of the system are identical for both the Bennett case and the Gaussian case: r_b=1 cm, $\omega_{pe}=9.9\times10^{10}$ rad/sec; $\omega_{ce}^z(\infty)=3.0\times10^{10}$ rad/sec; $n_b(0)/n_p(0)=0.01$; $\gamma=2$; $p_{th}/m_e c=0.1$.

Fig. 4 Example of a case where the azimuthal self magnetic field is greater than 10% of the applied field. Here a Gaussian density profile is used and r_b=2.0 cm; $\omega_{pe}=6.75\times10^{10}$ rad/sec; $\omega_{ce}^z(\infty)=3.0\times10^{10}$ rad/sec; $F_N=0$; $n_b(0)/n_p(0)=0.04$; $\gamma=2.0$; $p_{th}/m_e c=0.1$.

Fig. 5 Axial self-magnetic field, $B_z^s(r)$, as a function of radial position, r, for a Bennett density profile with various values of the beam radius, r_b. Note $B_z^s(r)=0$ for $r_b=\bar{r}_b=1.0$ cm. The other parameters of the system are the same as in Fig. 3 with $F_N=0.5$.

Fig. 6 Beam rotation frequency, $\omega_R(r)$, as a function of radial position, r, for a Bennett density profile with various values of the beam radius, r_b. Note $\omega_R(r)=0$ for $r_b=\tilde{r}_b=0.7$ cm. The other parameters of the system are the same as in Fig. 3 with $F_N=0.5$.

Fig. 7 Axial self-magnetic field, $B_s^s(r)$, as a function of radial position, R, for the case of a Gaussian density profile for various values of the beam radius r_b. Here $B_z^s(r)$ is nonzero for all r_b. The other parameters of the system are the same as in Fig. 3 with $F_N=0.5$.

Fig. 8 Beam rotation frequency, $\omega_R(r)$, as a function of radial position, r, for a Gaussian density profile with various values of the beam radius, R_b. Note: there is no nonrotating case for any R_b. The other parameters of the system are the same as in Fig. 3 with $F_N=0.5$.

Fig. 9 Azimuthal self magnetic field, $B_\theta^s(r)$, as a function of radial position, R, for a Bennett density profile. Here $F_N(r)=\bar{F}_N n_b(r)/n_b(0)$ for $\bar{F}_N=0.0$, 0.5 and 1.0. The other parameters of the system are the same as in Fig. 4.

Fig. 10 Azimuthal self magnetic field, $B_\theta^s(r)$, as a function of radial position, R, for a Gaussian density profile. Here $F_N(r)=\bar{F}_N n_b(r)/n_b(0)$ for $\bar{F}_N=0.0$, 0.5 and 1.0. The other parameters of the system are the same as in Fig. 4.

REFERENCES

*Research supported by ONR and NSF.

1. J. U. Guillory, Physics International Co. Report PIIR-14-72, Sept. 1972.
2. Ya. B. Fainberg, Plasma Phys. 4, 203 (1962).
3. A. T. Altyntsev, B. N. Breyzman, A. G. Eskov, O. A. Zolotivskii, V. I. Koroteev, R. X. Kurtmullaev, V. L. Masalov, D. D. Ryutov, and V. N. Semenov, in Plasma Physics and Controlled Nuclear Fusion Research (International Atomic Energy Agency, Vienna, 1971), Vol. 2, p. 309.
4. C. A. Kapetanakos and D. A. Hammer, Appl. Phys. Letters 23, 17 (1973).
5. G. C. Goldenbaum, W. F. Dove, K. A. Gerber, and B. G. Logan, Phys. Rev. Letters 32, 830 (1974).
6. L. I. Rudakov, Sov. Phys. JETP 32, 1134 (1971).
7. R. V. Lovelace and R. N. Sudan, Phys. Rev. Letters 27, 1256 (1971).
8. L. E. Thode and R. N. Sudan, Phys. Rev. Letters 30, 732 (1973).
9. M. Seidl, Phys. Fluids 13, 966 (1970).
10. C. A. Nyack and P. J. Christiansen, Plasma Phys. 17, 249 (1975).
11. B. B. Godfrey, W. R. Shanahan, and L. E. Thode, Phys. Fluids 18, 346 (1975).
12. L. S. Bogdankevich and A. A. Rukhadze, Sov. Phys. - USP 14, 163 (1971).
13. K. R. Chu and N. Rostoker, Phys. Fluids 16. 1472 (1973).
14. R. C. Davidson and B. H. Hui, Ann. Phys. 94, 209 (1975).
15. S. Bliman and A. Bouchoule, J. Appl. Phys. 38, 5065 (1967).
16. M. M. Shoucri and A. B. Kitsenko, Plasma Phys. 10, 699 (1968).
17. J. H. Adlam, Plasma Phys. 13, 329 (1971).

18. Z. Sedlacek, J. Plasma Phys. 5, 239 (1971); 6, 187 (1972).

19. P. F. Ottinger, University of Maryland Technical Report No. 76-054, 1976 (unpublished).

20. A. Nayfeh, Perturbation Methods (John Wiley and Sons, New York, 1973).

21. R. C. Davidson, private communication.

22. R. A. Mahaffey, University of Maryland, Preprint No. 503P028, 1975 (unpublished).

23. H. Davis, Introduction to Nonlinear Differential and Integral Equations (Dover, New York, 1962).

24. N. A. Krall and A. W. Trivelpiece, Principles of Plasma Physics (McGraw-Hill, New York, 1973), p. 395.

25. W. H. Bennett, Phys. Rev. 45, 890 (1934).

26. G. Benford and D. L. Book, in Advances in Plasma Physics (A. Simon and W. Thompson Eds., John Wiley and Sons, New York, 1971), Vol. 4, p. 125.

27. D. A. Hammer and N. Rostoker, Phys. Fluids 13, 1831 (1970).

28. G. Küppers, A. Salat, and H. K. Wimmel, Plasma Phys. 16, 317 (1974).

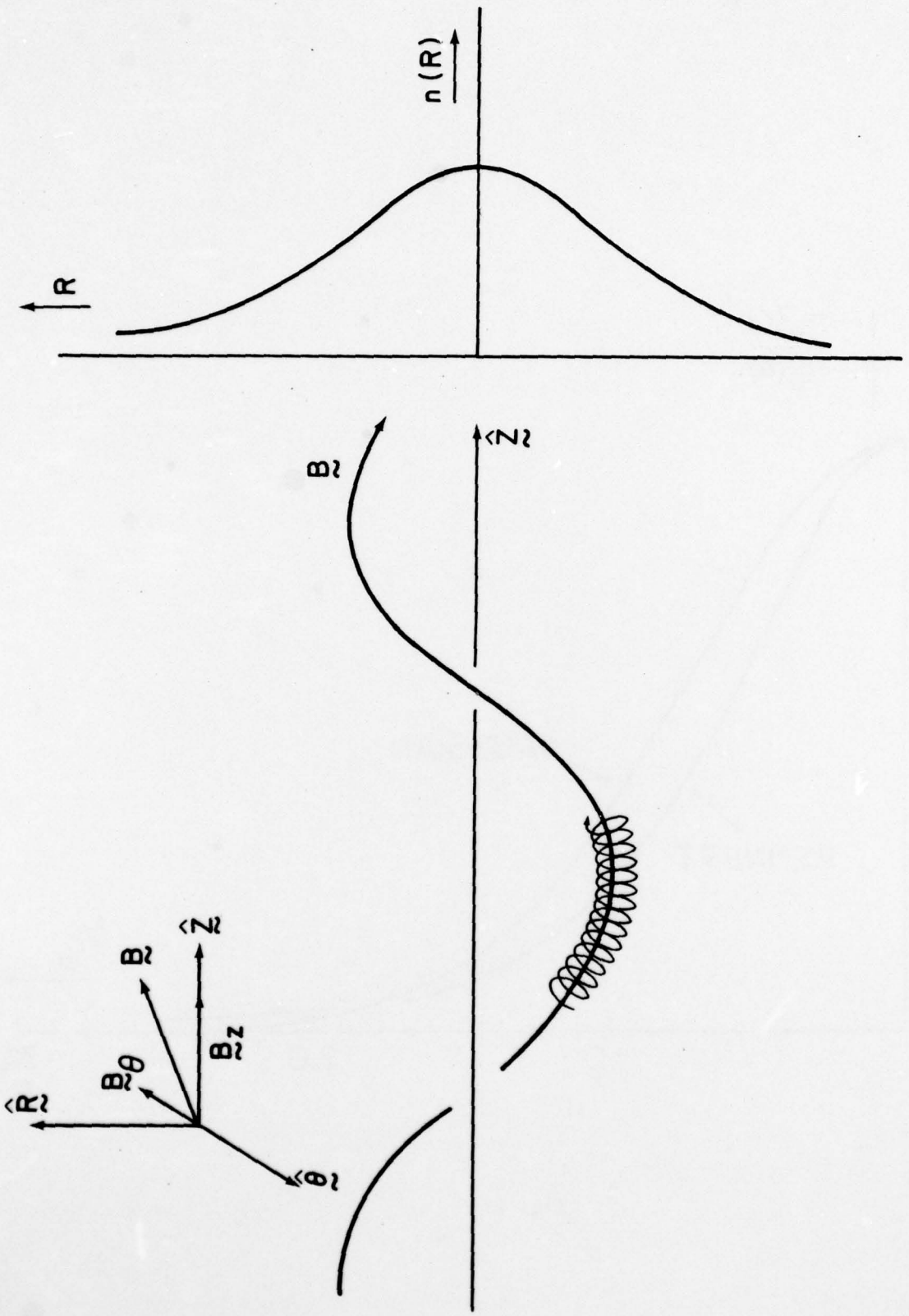

Fig. 1

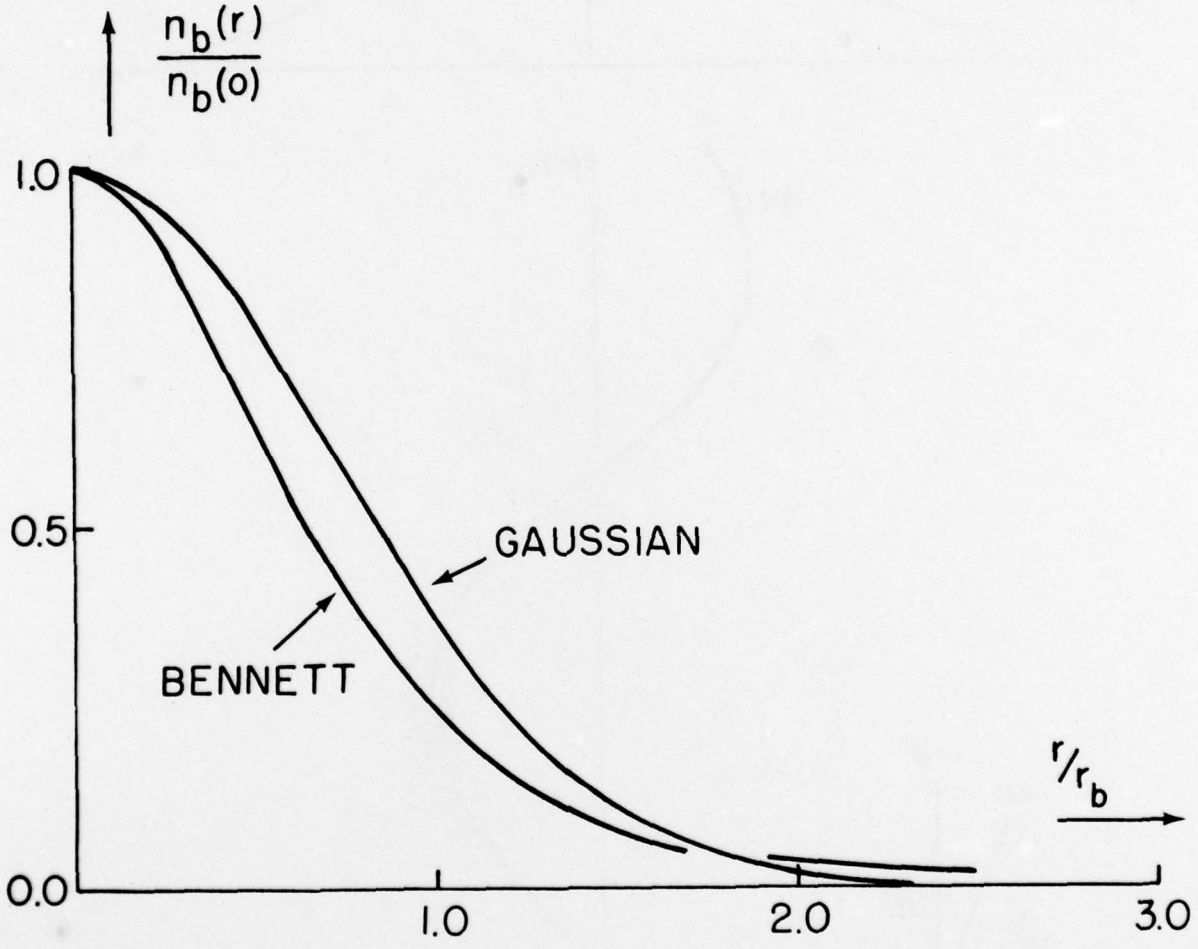

Fig. 2

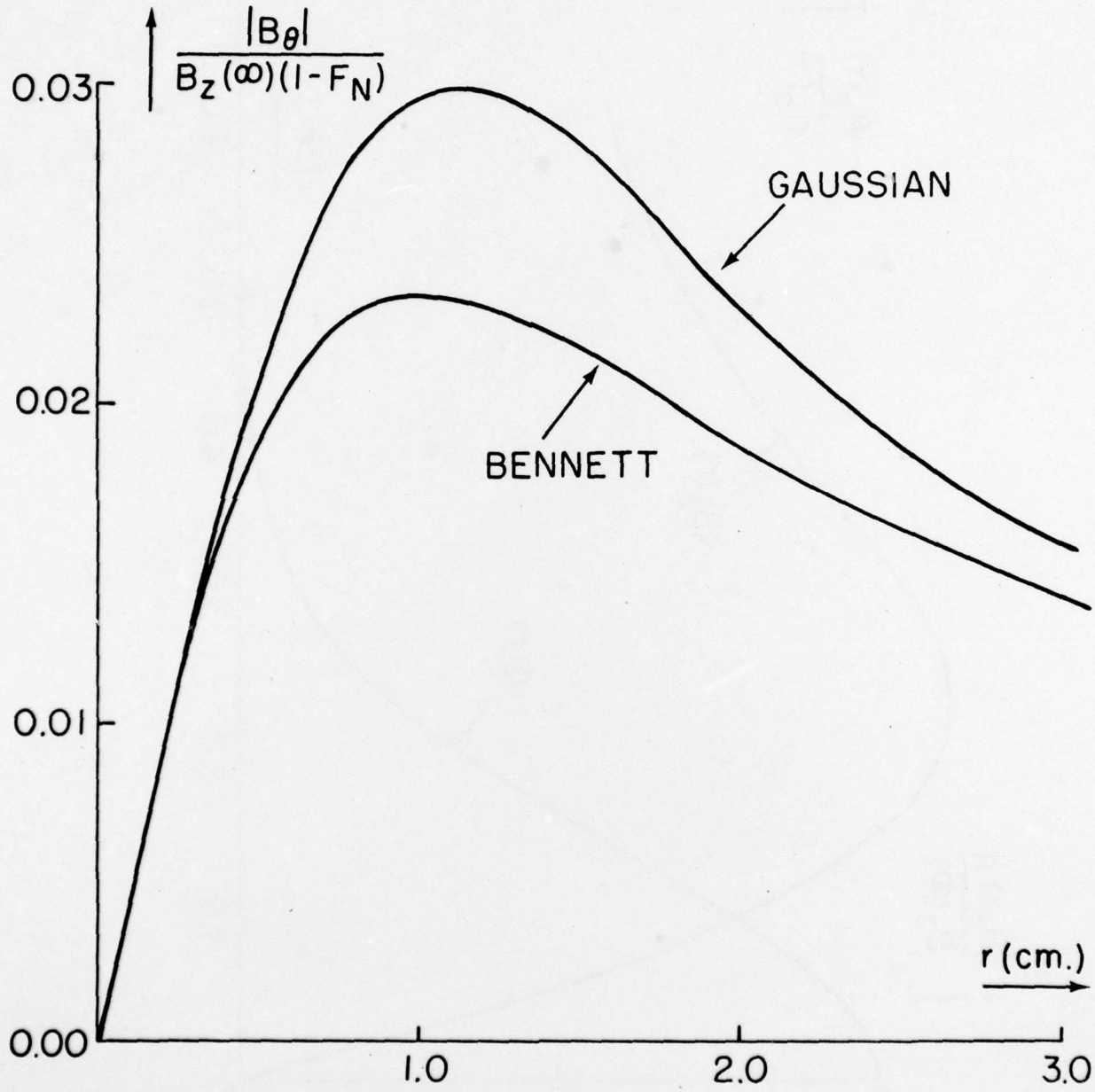
$\frac{|B_\theta|}{B_z(\infty)(1-F_N)}$
0.03
0.02
0.01
0.00
GAUSSIAN
BENNETT
r (cm.)
1.0
2.0
3.0

Fig. 3

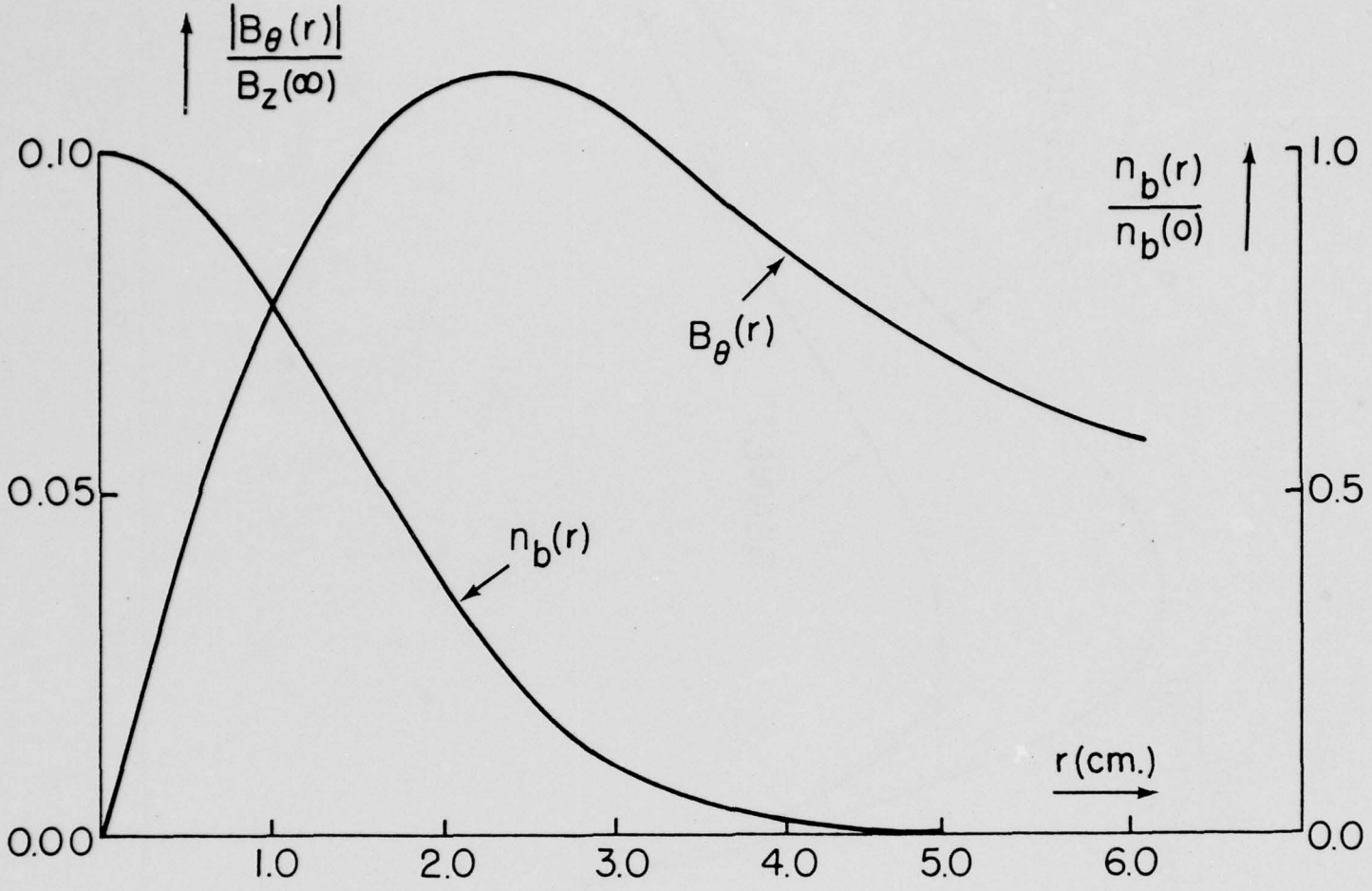
$\frac{|B_\theta(r)|}{B_z(\infty)}$
0.10
0.05
0.00
$B_\theta(r)$
$n_b(r)$
$\frac{n_b(r)}{n_b(o)}$
1.0
0.5
0.0
r(cm.)
1.0
2.0
3.0
4.0
5.0
6.0

Fig. 4

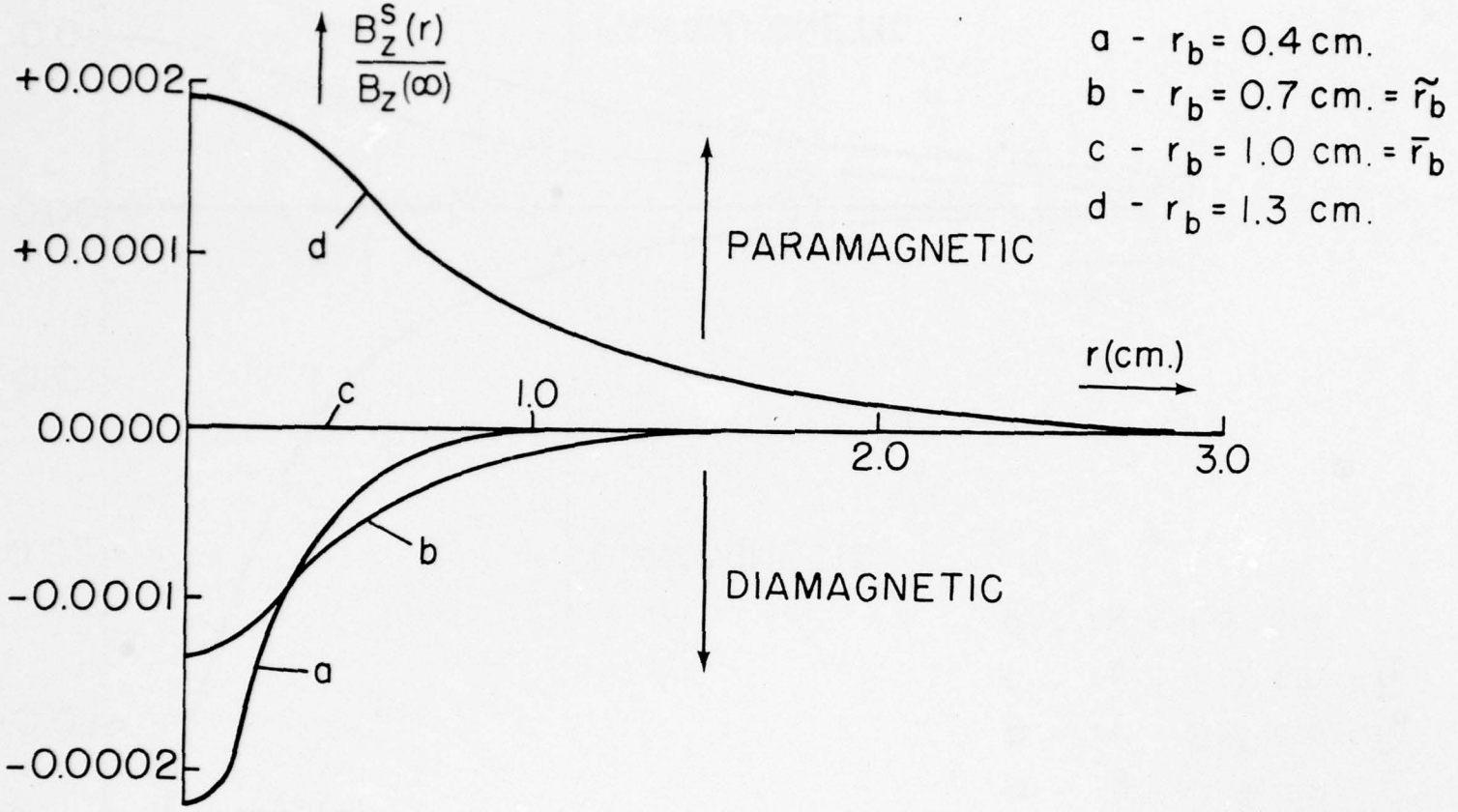
$B_z^s(r)$
$B_z(\infty)$
+0.0002
+0.0001
0.0000
-0.0001
-0.0002
d
c
b
a
1.0
2.0
3.0
r(cm.)
PARAMAGNETIC
DIAMAGNETIC
a - r_b = 0.4 cm.
b - r_b = 0.7 cm. = $\tilde{r}_b$
c - r_b = 1.0 cm. = $\bar{r}_b$
d - r_b = 1.3 cm.

Fig. 5

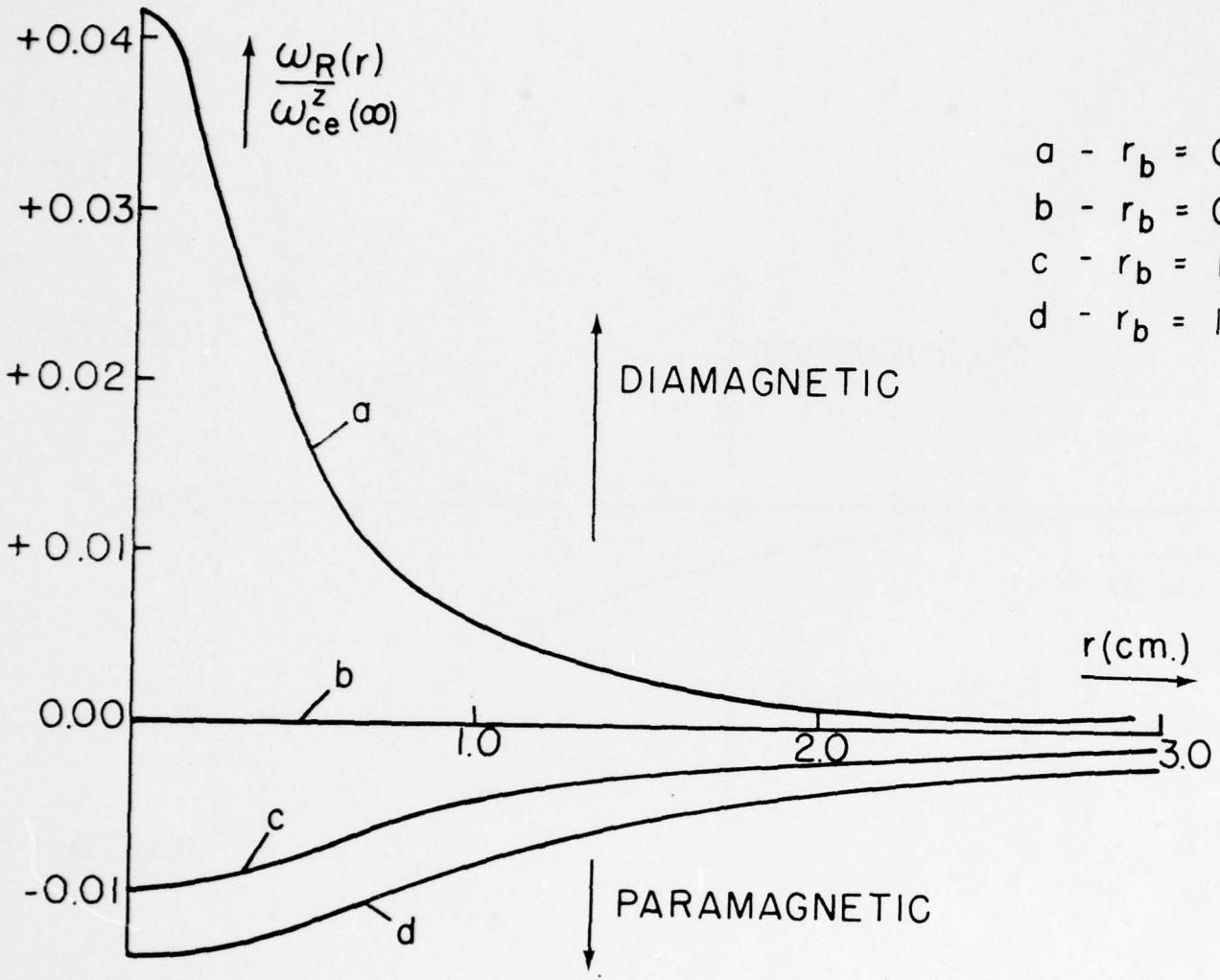
+0.04
+0.03
+0.02
+ 0.01
0.00
-0.01
$\frac{\omega_R(r)}{\omega_{ce}^2(\infty)}$
a - r_b = 0.4 cm.
b - r_b = 0.7 cm. = $\tilde{r}_b$
c - r_b = 1.0 cm. = $\bar{r}_b$
d - r_b = 1.3 cm.
DIAMAGNETIC
PARAMAGNETIC
r(cm.)
1.0
2.0
3.0
a
b
c
d

Fig. 6

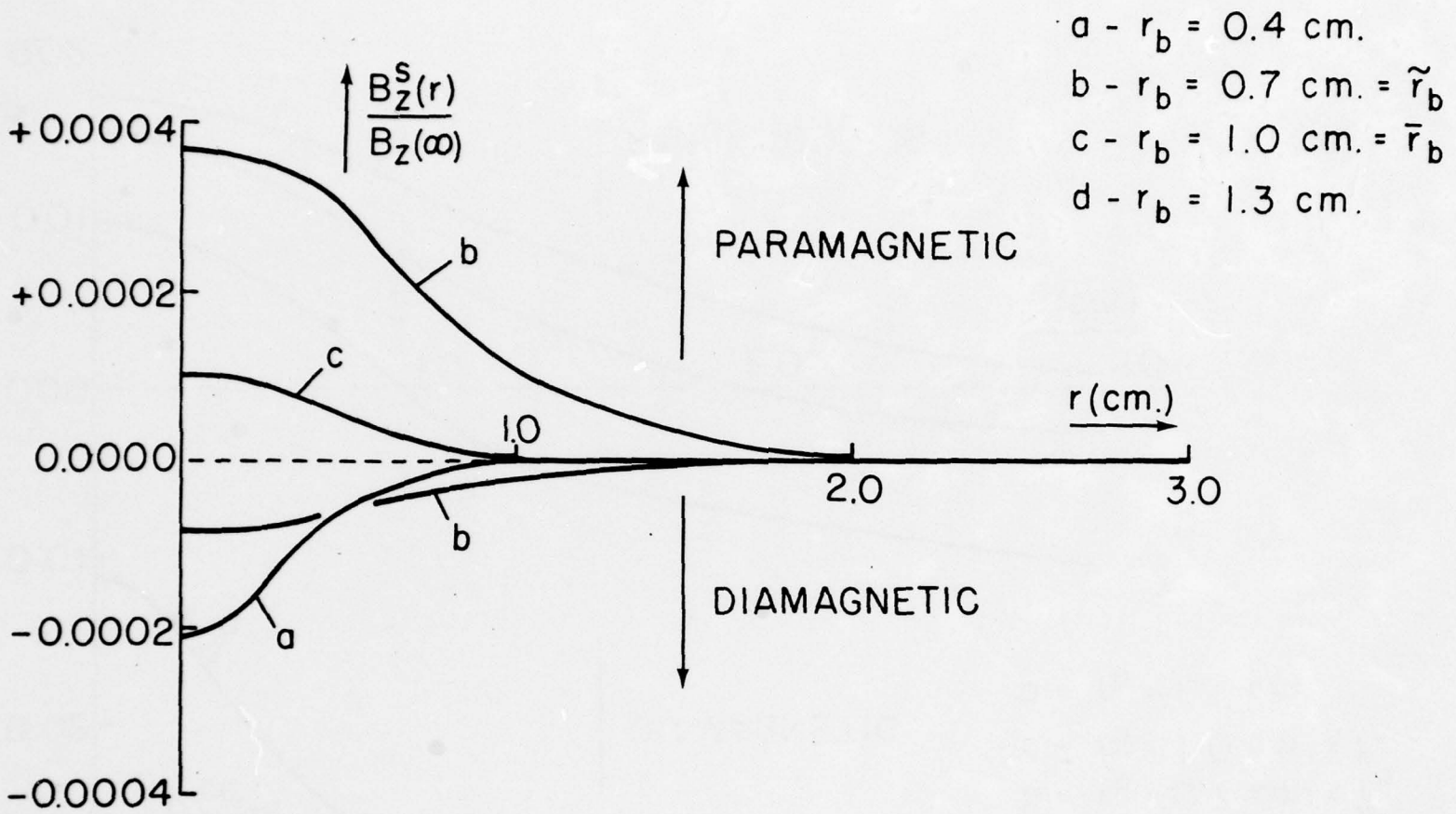
a - r_b = 0.4 cm.
b - r_b = 0.7 cm. = $\tilde{r}_b$
c - r_b = 1.0 cm. = $\bar{r}_b$
d - r_b = 1.3 cm.
$\frac{B_z^s(r)}{B_z(\infty)}$
+0.0004
+0.0002
0.0000
-0.0002
-0.0004
PARAMAGNETIC
DIAMAGNETIC
r(cm.)
1.0
2.0
3.0
a
b
c
b

Fig. 7

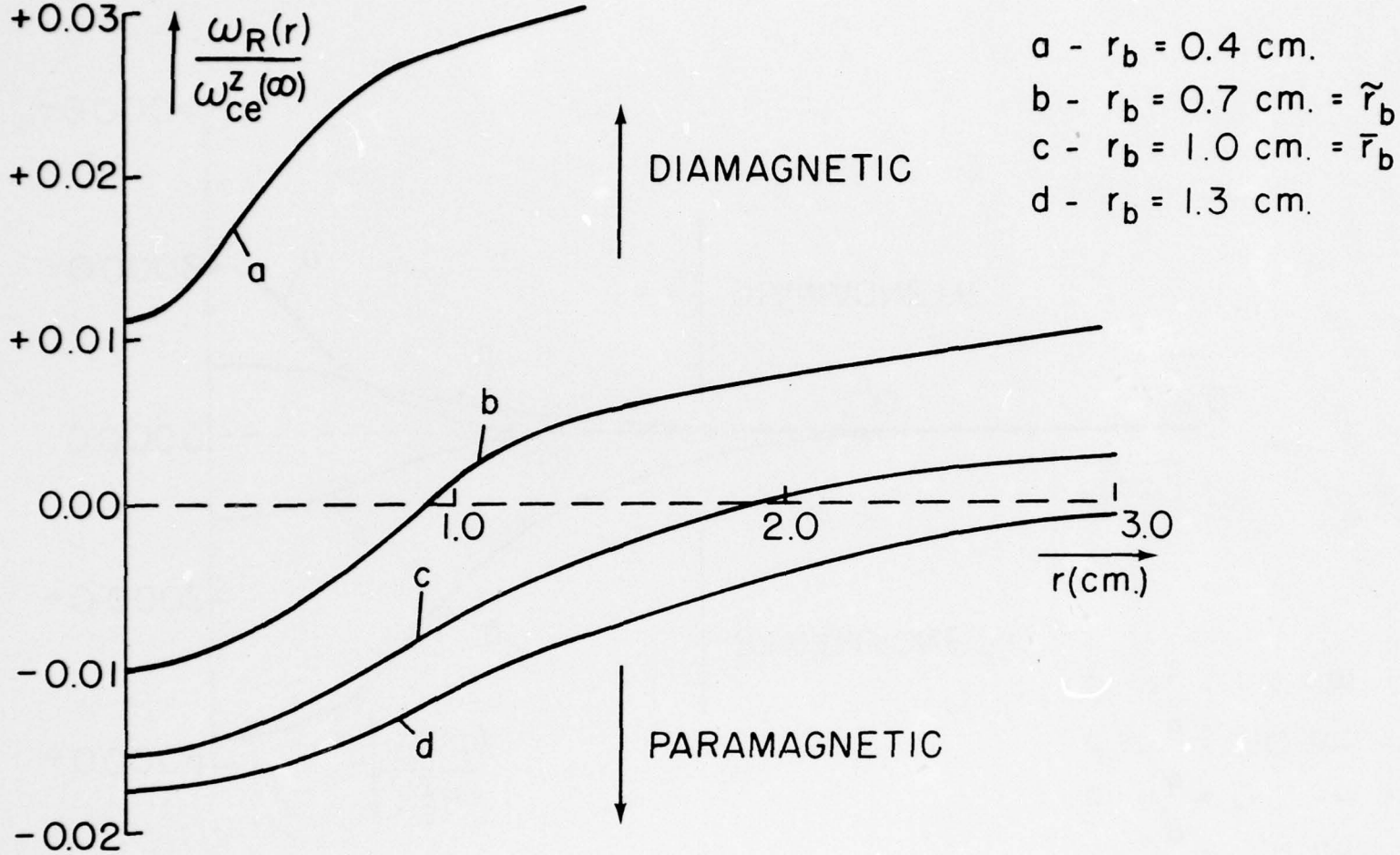
+0.03
+0.02
+0.01
0.00
-0.01
-0.02
$\frac{\omega_R(r)}{\omega_{ce}^z(\infty)}$
a
b
c
d
1.0
2.0
3.0
r(cm.)
DIAMAGNETIC
PARAMAGNETIC
a - r_b = 0.4 cm.
b - r_b = 0.7 cm. = $\tilde{r}_b$
c - r_b = 1.0 cm. = $\bar{r}_b$
d - r_b = 1.3 cm.

Fig. 8

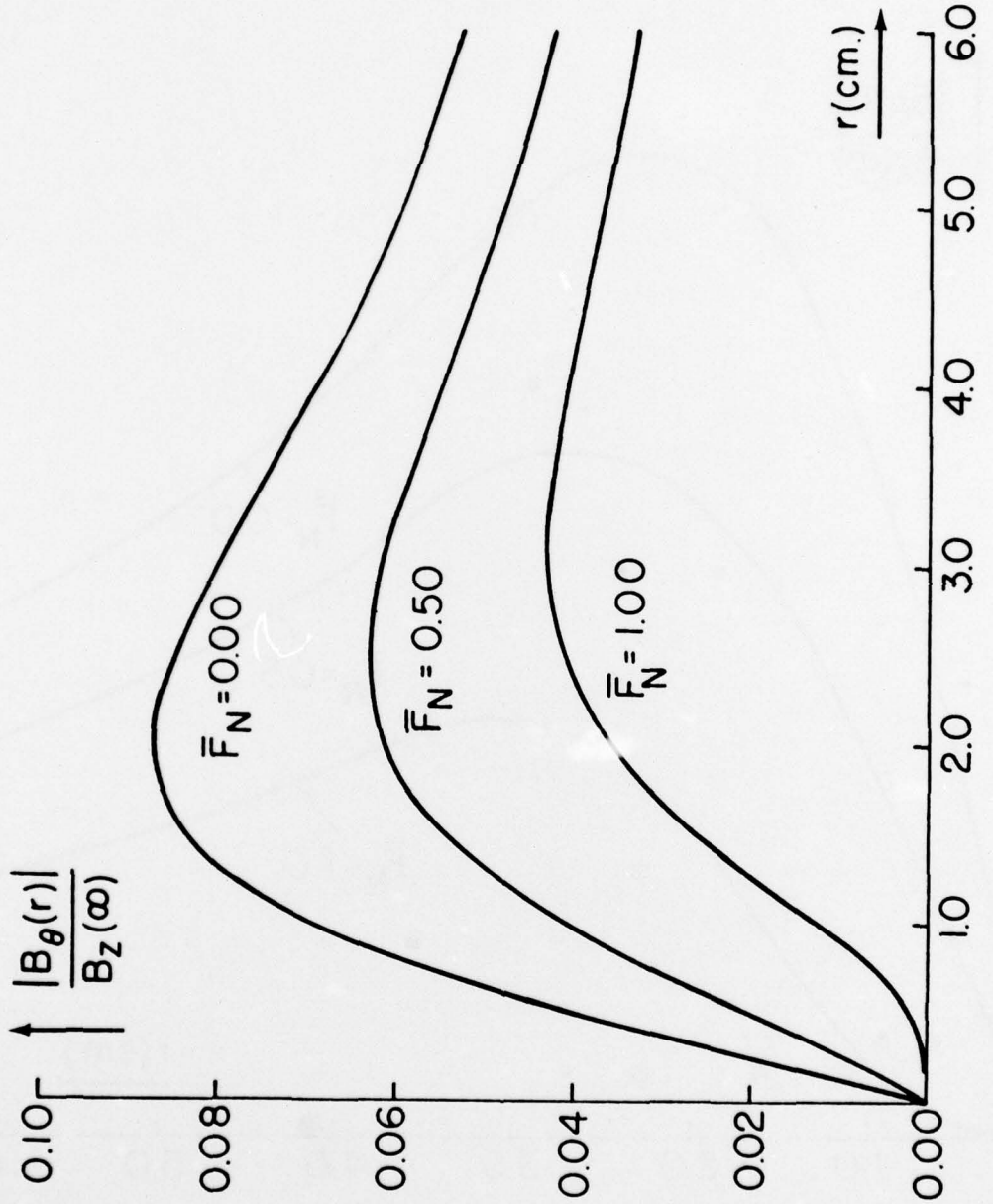
$\frac{|B_\theta(r)|}{B_z(\infty)}$
0.10
0.08
0.06
0.04
0.02
0.00
$\bar{F}_N$=0.00
$\bar{F}_N$= 0.50
$\bar{F}_N$= 1.00
1.0
2.0
3.0
4.0
5.0
6.0
r(cm.)

Fig. 9

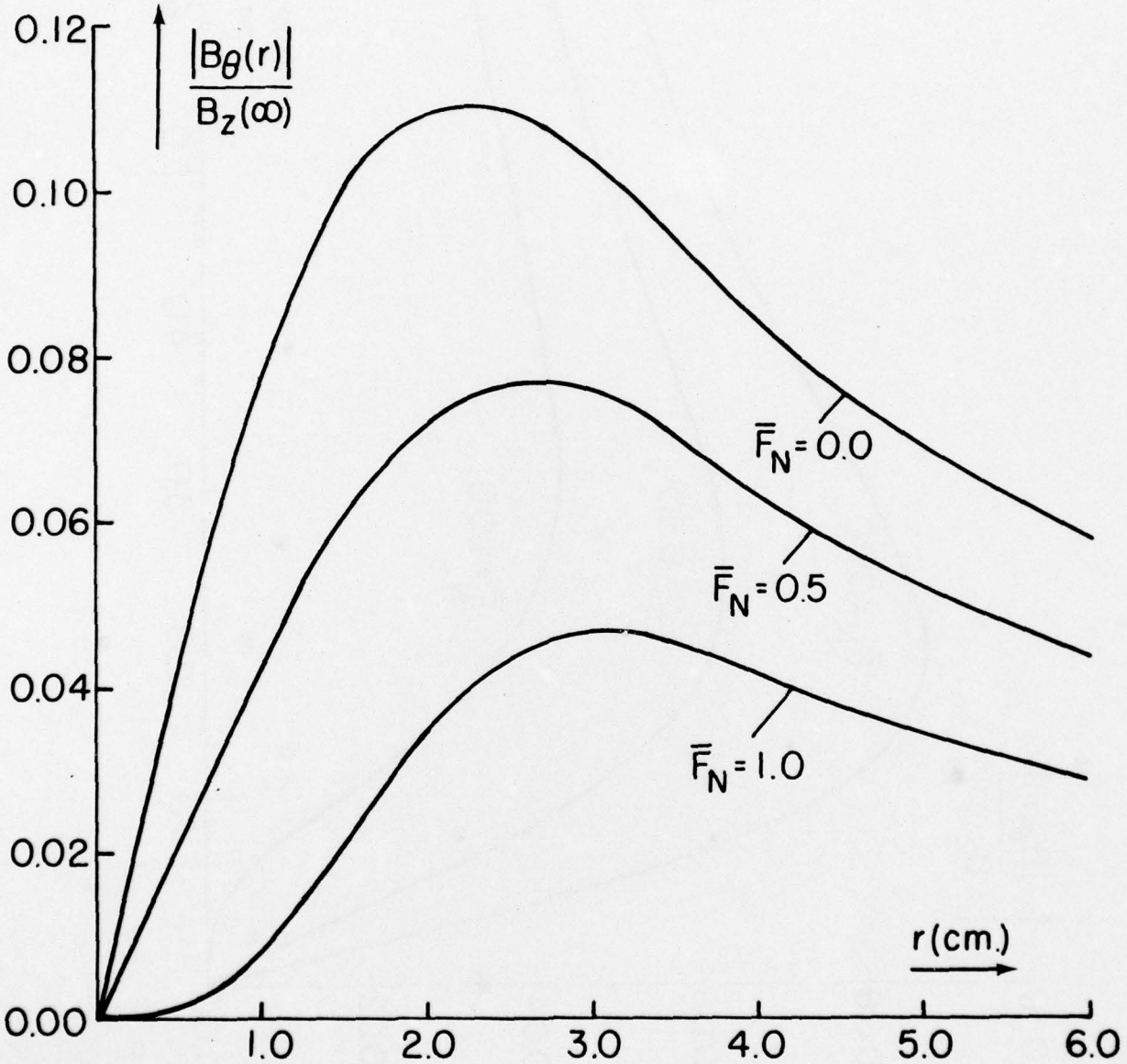
0.12
0.10
0.08
0.06
0.04
0.02
0.00
$\frac{|B_\theta(r)|}{B_z(\infty)}$
$\bar{F}_N = 0.0$
$\bar{F}_N = 0.5$
$\bar{F}_N = 1.0$
r(cm.)
1.0
2.0
3.0
4.0
5.0
6.0

Fig. 10